MECHANICAL

TECHNOLOGY

INCORPORATED

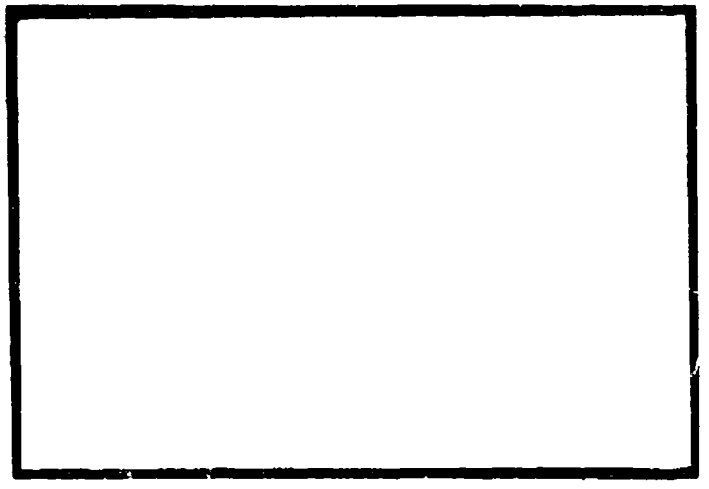

MECHANICAL TECHNOLOGY INCORPORATED
968 Albany Shaker Road
Latham, New York 12110

MTI 69TR23

REFINED SOLUTION OF PNEUMATIC HAMMER INSTABILITY OF INHERENTLY COMPENSATED HYDROSTATIC THRUST GAS BEARINGS

by

T. Chiang
C.H.T. Pan

March 1969

NO. MTI 69TR23

DATE: March 1969

TECHNICAL REPORT

REFINED SOLUTION OF PNEUMATIC HAMMER INSTABILITY OF INHERENTLY COMPENSATED HYDROSTATIC THRUST GAS BEARINGS

by
T. Chiang
C.H.T. Pan

T. Chiang C.H.T. Pan

Author (s)

Walter A Simons

Approved

Approved

Prepared under

Contract Nonr-3730(00)

Task NR 062-317/1-9-68

Prepared for

Department of Defense
Atomic Energy Commission
National Aeronautics and Space Administration

Administered by

Office of Naval Research
Department of the Navy

MTI
MECHANICAL TECHNOLOGY INCORPORATED

968 ALBANY - SHAKER ROAD — LATHAM, NEW YORK — PHONE 785-0922

TABLE OF CONTENTS

ABSTRACT

An externally-pressurized gas thrust bearing was analyzed for both static and dynamic characteristics. The bearing is fed through an inherently compensated restrictor into a shallow packet. The analysis gave special attentions to the significance of the recent finding of restrictor flow (Ref. 4), the trade-off consideration between static stiffness and stability margin, and the effects of the pocket depth.

1. INTRODUCTION

Externally pressurized gas bearings have been used in many engineering devices. It is well known that in order for the bearing to have relatively large load capacity and stiffness it is desirable to have recessed pockets immediately after the feeding holes. This causes the externally pressurized gas bearings to be susceptible to pneumatic hammer instability. Analytical investigations on this subject were made in References 1, 2 and 3.

In conventional analyses of externally pressurized bearings, nozzle equations are used in calculating the flow across a restrictor. The dynamic pressure head resulting from expansion through the restrictor is assumed to be completely lost when entering the bearing film. This, however, is not true as reported in References 4 and 5; a measurement of pressure at the restrictor exit indicates that there is considerable pressure recovery. It was shown that the pressure loss coefficient can be correlated with the Reynolds' number (Ref. 4); a linear relationship is chosen for simplicity.

A simple thrust plate with a feeding hole at the center and a recessed pocket immediately after it, is to be analyzed. The same bearing configuration was previously analyzed in Ref. 12 using the above pressure loss coefficient correlation for the restrictor flow and the Reynolds' equation for the bearing film but assuming a uniform pressure in the pocket. This will be modified in the present analysis by writing another Reynolds' equation for the recessed pocket. This modification is particularly significant when the pocket is shallow which is usually the case as the result of a trade-off consideration between stiffness and stability. Perturbation analysis for small oscillation about the equilibrium position will be performed. Based on the perturbation analysis, dynamic bearing stiffness and damping coefficients can be calculated. Using the stability analysis of Ref. 6, stability maps are constructed. The results using the nozzle equation are also presented for comparison.

2. ANALYSIS

The configuration of an inherently compensated, hydrostatic, circular, thrust bearing is schematically shown in Fig. 1. Gas at supply pressure p_s is led through the feeding hole with diameter d_f, into the recessed pocket before entering the bearing film. For a circular bearing it is convenient to use the polar coordinates. If we further assume circular symmetry, i.e. no misalignment, then the radial coordinate, r, is the only space variable required to describe the flow and the pressure distribution. In order to facilitate a dynamic analysis let us allow the bearing to have small axial vibrations about its equilibrium position and express the bearing film thickness as

$$h = C + \epsilon \cos \tau \tag{2.1}$$

or in dimensionless form

$$\bar{h} = 1 + \bar{\epsilon} \cos \tau \tag{2.2}$$

where

$$\begin{aligned} \bar{h} &= h/C \\ \bar{\epsilon} &= \epsilon/C \\ C &= \text{equilibrium film thickness} \\ \tau &= \omega t = \text{dimensionless time} \\ \omega &= \text{frequency of vibration} \end{aligned} \tag{2.3}$$

We have assumed that the vibrations are purely sinusoidal. Note that $\bar{\epsilon}$, the normalized amplitude of vibration, is a small number.

The well-known time-dependent, isothermal Reynolds' equation can be written in dimensionless form,

$$\frac{1}{\bar{r}} \frac{\partial}{\partial \bar{r}} \left[(\bar{r}) \ (\bar{h} + \bar{h}_R)^3 \ \bar{p} \ \frac{\partial \bar{p}}{\partial \bar{r}} \right] = \sigma \frac{\partial}{\partial \tau} \left[\bar{p} \ (\bar{h} + \bar{h}_R) \right] \ ; \ \bar{r}_F < \bar{r} < \bar{r}_R \tag{2.4}$$

$$\frac{1}{\bar{r}} \frac{\partial}{\partial \bar{r}} \left(\bar{r}\, \bar{h}^3\, \bar{p}\, \frac{\partial \bar{p}}{\partial \bar{r}} \right) = \sigma \frac{\partial}{\partial \tau} \left(\bar{p}\, \bar{h} \right) \; ; \quad \bar{r}_R < \bar{r} < 1 \tag{2.5}$$

where

$$\begin{aligned} \bar{r} &= r/R \\ \bar{p} &= p/p_a \\ \sigma &= \frac{12\mu\omega}{p_a} \left(\frac{R}{C} \right)^2 = \text{squeeze number} \\ \bar{h}_R &= \frac{h_R}{C} = \text{dimensionless depth of recessed pocket} \\ \bar{r}_F,\ \bar{r}_R &= \text{dimensionless radii of the feeding hole and the recessed pocket, see Fig. 1} \end{aligned} \tag{2.6}$$

It is seen that the pressure distributions of both the recessed pocket ($\bar{r}_F < \bar{r} < \bar{r}_R$) and the film ($\bar{r}_R < \bar{r} < 1$) are governed by the respective Reynolds' equations (2.4) and (2.5).

The boundary condition at the outer edge is

$$\bar{p} = 1 \quad \text{at} \quad \bar{r} = 1 \tag{2.7}$$

The pressures at $\bar{r}_F$ and $\bar{r}_R$ are designated as follows:

$$\begin{aligned} &\text{at } \bar{r} = \bar{r}_F, \quad \bar{p} = \bar{p}_F \\ &\text{at } \bar{r} = \bar{r}_{R-}, \quad \bar{p} = \bar{p}_E \\ &\text{at } \bar{r} = \bar{r}_{R+}, \quad \bar{p} = \bar{p}_R \end{aligned} \tag{2.8}$$

Note that there is a discontinuity in pressure at $\bar{r} = \bar{r}_R$. The pressures, $\bar{p}_F$, $\bar{p}_E$ and $\bar{p}_R$, are yet unknown. Additional pressure flow relationships across the inlet restriction at $\bar{r} = \bar{r}_F$ and at $\bar{r} = \bar{r}_R$ are required for the solution. In the literature (Refs. 1, 2, 3) the well-known nozzle formula is used to calculate the expansion of air from p_s to p_F and from p_E to p_R. If the pressure calculated according to the nozzle equation are accepted, one automatically assumes that the velocity head resulting from expansion through the nozzle is

completely lost. This is not so because part of the velocity head is recovered as indicated by Ref. 4 and 5. In fact, a correlation formula for the pressure drop and the velocity head was obtained by Vohr (Ref. 4). In the following, both methods of approach, the Vohr's correlation formular and the nozzle equation, will be used for the analysis.

Using Vohr's Experimental Correlation

The experimental correlation of Vohr (Ref. 4) shows that the pressure drop at the entrance is related to the velocity head by

$$(\Delta p)_{ent} = K' \; p_{dyn} \tag{2.9}$$

where p_{dyn} is the dynamic head expressed in the form of a pressure. The film entrance loss coefficient, K', is correlated with $\bar{R}_e$ (or $\dot{m}/\pi r\mu$) in Ref. 4, which is reproduced in Fig. 2. For all practical purposes, a linear relationship between K' and $\bar{R}_e$ is satisfactory. Hence,

$$K' = K \bar{R}_e = K \frac{\dot{m}}{\pi r \mu} \tag{2.10}$$

Note that K is a constant, and

$$K = 0.33 \times 10^{-3} \tag{2.11}$$

Applying the above formulation to the restriction at $\bar{r} = \bar{r}_F$, we have

$$p_s - p_F = K \cdot \frac{\dot{m}_F}{\pi r_F \mu} \; p_{dyn} \tag{2.12}$$

Here, the velocity head p_{dyn} can be obtained by

$$p_{dyn} = p_s - p_e \tag{2.13}$$

It is to be noted that p_e is a fictitious pressure through an isentropic expansion which will carry the gas to its downstream Mach numbers corresponding to $\dot{m}_F$. This can be realized by noting that

$$\dot{m}_F = \rho_e V_e a_e \tag{2.14}$$

where ρ_e and V_e are the density and velocity corresponding to p_e, and a_e is the flow cross-sectional area. Observe the following identity

$$\frac{\dot{m}_F}{C^* a_\delta \rho_s} = \frac{\rho_e}{\rho_s} \frac{V_e}{C^*} = \frac{\rho_e}{\rho_s} M_e^* \tag{2.15}$$

$$\left.\begin{aligned} &\text{where } C^* = \text{the speed of sound at sonic velocity} \\ &M_e^* = \frac{V_e}{C^*} = \text{Mach number with respect to } C^* \end{aligned}\right] \tag{2.16}$$

Since both ρ_e/ρ_s and M_e^* are function of Mach number only (for the ficticious isentropic expansion), let us denote

$$f_e = f(M_e) = \frac{\rho_e}{\rho_s} M_e^* \tag{2.17}$$

Then, from Eq. (2.15)

$$\left.\begin{aligned} f_e &= \frac{\dot{m}_F}{C^* a_e \rho_s} = \frac{\rho_e}{\rho_s} M_e^* \\ a_e &= 2\pi r_F (h + h_R) \end{aligned}\right] \tag{2.18}$$

For a given M_e, the quantities ρ_e/ρ_s and M_e^* can be determined with the aid of a gas table. (Ref. 10). Then $\dot{m}_F$ can be easily calculated from (2.18). Note that

$$C^* = \sqrt{\frac{2\gamma}{\gamma+1} \mathcal{R} T} \tag{2.19}$$

where

$$\left.\begin{aligned} &\gamma = \text{ratio of specific heats} \\ &\mathcal{R} = \text{gas constant} = 2.47 \times 10^5 \ \frac{\text{in}^2}{\text{sec}^2 \cdot \text{R}} \ \text{for air} \\ &T = \text{absolute temperature of bearing} \end{aligned}\right] \tag{2.20}$$

Conversely, once $\dot{m}_F$ is known, M_e can be determined, which in turn yields p_e/p_s. Similarly, the loss at the second restriction ($r = r_R$) is

$$p - p_R = K \frac{\dot{m}_R}{\pi r_R \mu} \tag{2.21}$$

Now, p_E is obviously the supply pressure for this restrictor and p_g is the pressure resulting from a ficticious isentropic expansion. Corresponding to (2.18), we have

$$f_g = f(M_g) = \frac{\rho_g}{\rho_e} M_g^* = \frac{\dot{m}_R}{C^* a_g \rho_E} \tag{2.22}$$

$$a_g = 2\pi r_R h$$

In solving the Reynolds' equations (2.4) and (2.5) with small periodic variations of the gap about the equilibrium position, we write in complex form,

$$\bar{h} = 1 + \bar{\epsilon} e^{i\tau} \tag{2.23}$$

and expand the dimensionless pressure

$$\bar{p} = \bar{p}_o + \bar{\epsilon} \bar{p}_1 e^{i\tau} \tag{2.25}$$

$$\dot{m}_F = \dot{m}_{Fo} + \bar{\epsilon} \dot{m}_{F1} e^{i\tau} \tag{2.26}$$

The mass flow rates $\dot{m}_F$ and $\dot{m}_R$ can be expressed in terms of pressure gradient as follows:

$$\dot{m}_F = -2\pi r_F \frac{(h + h_R)^3}{12\mu} \left[\rho \frac{\partial p}{\partial r}\right]_{r_F} \tag{2.27}$$

$$\dot{m}_R = -2\pi r_R \frac{h^3}{12\mu}\left[\rho \frac{\partial p}{\partial r}\right]_{r_R} \tag{2.28}$$

Thus, we have

$$\dot{m}_{Fo} = -\pi \bar{r}_F P_a^2 \frac{(C + h_R)^3}{12\mu \mathcal{R}T} \left.\frac{\partial \bar{p}_o^2}{\partial \bar{r}}\right|_{\bar{r}_F} \tag{2.29}$$

$$\dot{m}_{F1} = \dot{m}_{Fo}\left[\frac{3}{1 + \bar{h}_R} + 2 \left.\frac{\frac{\partial(\bar{p}_o \bar{p}_1)}{\partial \bar{r}}}{\partial \bar{p}_o^2/\partial \bar{r}}\right|_{\bar{r}_F}\right] \tag{2.30}$$

and

$$\dot{m}_{Ro} = \pi \bar{r}_R P_a^2 \frac{C^3}{12\mu \mathcal{R}T} \left.\frac{\partial \bar{p}_o^2}{\partial \bar{r}}\right|_{\bar{r}_R} \tag{2.31}$$

$$\dot{m}_{R1} = \dot{m}_{Ro}\left[3 + 2 \left.\frac{\frac{\partial(\bar{p}_o \bar{p}_1)}{\partial \bar{r}}}{\frac{\partial \bar{p}_o^2}{\partial \bar{r}}}\right|_{\bar{r}_R}\right] \tag{2.32}$$

From (2.12) and (2.13) it is clear that

$$p_s - p_{Fo} - \bar{\epsilon}\, p_{F1}\, e^{i\tau}$$

$$= K \frac{\dot{m}_{Fo} + \bar{\epsilon}\, \dot{m}_{F1}\, e^{i\tau}}{\pi r_F \mu}\left[p_s - p_{eo} - \bar{\epsilon}\, p_{e1}\, e^{i\tau}\right]$$

Hence,

$$p_s - p_{Fo} = K \frac{\dot{m}_o}{\pi r_F \mu}(p_s - p_{eo}) \tag{2.33}$$

$$- \frac{p_{F1}}{p_s - p_{Fo}} = \frac{\dot{m}_{F1}}{\dot{m}_o} - \frac{p_{e1}}{p_s - p_{eo}} \tag{2.34}$$

Similarly, from (2.21)

$$p_{Eo} - p_{Ro} = K \frac{\dot{m}_{Ro}}{\pi r_R \mu} (p_{Eo} - p_{go}) \tag{2.35}$$

and

$$\frac{p_{E1} - p_{R1}}{p_{Eo} - p_{Ro}} = \frac{\dot{m}_{R1}}{\dot{m}_o} + \frac{p_{E1} - p_{g1}}{p_{Eo} - p_{go}} \tag{2.36}$$

Note that we have already used the steady-state mass conservation relationship.

$$\dot{m}_{Ro} = \dot{m}_{Fo} = \dot{m}_o \tag{2.37}$$

Before we go any further, let us observe that there is a singular point in Eq. (2.4) at $\bar{r} = o$. Although $\bar{r}$ is never equal to zero ($\bar{r} > \bar{r}_F > o$), the gradients may become very steep near $\bar{r} = \bar{r}_F$ if $\bar{r}_F$ is small in comparison to unity. It is therefore convenie t to make the following coordinate transformation.

$$\frac{d\bar{r}}{\bar{r}} = d\xi \tag{2.38}$$

or $\ln \bar{r} = \xi$ (2.39)

and $\bar{r} \frac{\partial}{\partial \bar{r}} = \frac{\partial}{\partial \xi}$ (2.40)

Under the transformed coordinate, Eqs. (2.4) and (2.5) become

$$\frac{\partial}{\partial \xi} \left[(\bar{h} + \bar{h}_R)^3 \bar{p} \frac{\partial \bar{p}}{\partial \xi} \right] = e^{2\xi} \sigma \frac{\partial}{\partial \tau} \left[\bar{p} (\bar{h} + \bar{h}_R) \right] \quad ; \quad \xi_F < \xi < \xi_R . \tag{2.41}$$

$$\frac{\partial}{\partial \xi}\left[\bar{h}^3\ \bar{p}\ \frac{\partial \bar{p}}{\partial \xi}\right] = e^{2\xi}\ \sigma\ \frac{\partial}{\partial \tau}\ (\bar{p}\ \bar{h})\ ;\ \xi_{R+} < \xi < o \tag{2.42}$$

with boundary conditions

$$\left.\begin{array}{ll} \text{at } \xi = \xi_F & \bar{p} = \bar{p}_F \\ \text{at } \xi = \xi_{R-} & \bar{p} = \bar{p}_E \\ \text{at } \xi = \xi_{R+} & \bar{p} = \bar{p}_R \\ \text{at } \xi = o & \bar{p} = 1 \end{array}\right\} \tag{2.43}$$

where $\xi_F = \ln \bar{r}_F$ etc. (2.44)

Applying perturbation to (2.41) and (2.42), we obtain

$$\left.\begin{array}{ll} \frac{d}{d\xi}\left[\frac{d\bar{p}_o}{d\xi}^2\right] = o & (2.45a) \\ \frac{\partial}{\partial \xi}\left[\frac{\partial(\bar{p}_o \bar{p}_1}{\partial \xi}\right] = e^{2\xi}\ \frac{\sigma}{(1+\bar{h}_R)^3}\ i\left[\bar{p}_o + (1+\bar{h}_R)\ \bar{p}_1\right] & (2.45b) \end{array}\right\} (\xi_F < \xi < \xi_{R-})$$

$$\left.\begin{array}{ll} \frac{d}{d\xi}\left[\frac{d\bar{p}_o}{d\xi}^2\right] = o & (2.46a) \\ \frac{\partial}{\partial \xi}\left[\frac{\partial(\bar{p}_o \bar{p}_1)}{\partial \xi}\right] = e^{2\xi}\ \sigma\ i\ \left[\bar{p}_o + \bar{p}_1\right] & (2.46b) \end{array}\right\} (\xi_{R+} < \xi < o)$$

Steady-State Solution

The solutions of Eqs. (2.45a) and (2.46A) satisfying boundary conditions (2.43) are

$$\bar{p}_o = \left[\frac{\xi_F\ \bar{p}_{Eo}^{\ 2} - \xi_R\ \bar{p}_{Fo}^{\ 2}}{\xi_F - \xi_R} + \frac{\bar{p}_{Fo}^{\ 2} - \bar{p}_{Eo}^{\ 2}}{\xi_F - \xi_R}\ \xi\right]^{1/2} \qquad \xi_F < \xi < \xi_{R-} \tag{2.47}$$

$$\bar{p}_o = \left[1 + (\bar{p}_{Ro}^2 - 1)\frac{\xi}{\xi_R}\right]^{1/2} \qquad \xi_{R+} < \xi < o \qquad (2.48)$$

The quantities $\bar{p}_{Fo}$, $\bar{p}_{Eo}$ and $\bar{p}_{Ro}$ are to be determined by mass conservation and pressure drop relationships as follows:

From (2.39) and (2.31)

$$\dot{\bar{m}}_o = -\frac{1}{2}\,\frac{(1+\bar{h}_R)^3}{\Lambda_s^* \bar{p}_s^2}\,\frac{\bar{p}_{Fo}^2 - \bar{p}_{Eo}^2}{\xi_F - \xi_R} \qquad (2.49)$$

$$\dot{\bar{m}}_o = -\frac{1}{2}\,\frac{1}{\Lambda_s^* \bar{p}_s^2}\,\frac{\bar{p}_{Ro}^2 - 1}{\xi_R} \qquad (2.50)$$

where $$\dot{\bar{m}}_o = \frac{\dot{m}_o}{\rho_s \sqrt{RT}\; 2\pi r_F (C + h_R)} = \text{dimensionless mass flux} \qquad (2.51)$$

$$\Lambda_s^* = \frac{12\mu\sqrt{RT}\, r_F (C + h_R)}{p_s C^3}$$

$$= \text{feeding parameter} \qquad (2.52)$$

and from (2.33) and (2.35)

$$\bar{p}_s - \bar{p}_{Fo} = K \dot{\bar{m}}_o \frac{24}{\Lambda_s^*}(1+\bar{h}_R)^2 \frac{r_F}{C}(\bar{p}_s - \bar{p}_{Eo}) \qquad (2.53)$$

$$\bar{p}_{Eo} - \bar{p}_{Ro} = K \dot{\bar{m}}_o \frac{24}{\Lambda_s^*}(1+\bar{h}_R)^2 \frac{r_F^2}{C r_R}(\bar{p}_{Eo} - \bar{p}_{go}) \qquad (2.54)$$

The dimensionless mass flux has a maximum when the flow is choked. In most circumstances, the choking occurs at the first restrictor because the area is smaller than that of the second restrictor. Then, from Eq. (2.51) we have for $\gamma = 1.4$,

$$(\dot{\bar{m}}_o)_{\text{choked}} = \frac{\rho}{\rho_s}\sqrt{\frac{2\gamma}{\gamma+1}} = 0.68$$

Two additional equations are obtained from Eqs. (2.18) and (2.22),

$$f_e = \dot{\bar{m}}_o \sqrt{\frac{\gamma - 1}{2\gamma}} \tag{2.55}$$

$$f_g = \frac{\bar{p}_s}{\bar{p}_{Eo}} \frac{r_F}{r_R} (1 + \bar{h}_R) \dot{\bar{m}}_o \sqrt{\frac{\gamma-1}{2\gamma}} \tag{2.56}$$

Recall that f_e and f_g are implicit functions of $\bar{p}_{eo}$ and $\bar{p}_{go}$ respectively. Thus, we have six equations, (2.49), (2.50), (2.53), (2.54), (2.55) and (2.56) to solve for six unknown quantities, $\dot{\bar{m}}_o$, $\bar{p}_{Fo}$, $\bar{p}_{Eo}$, $\bar{p}_{Ro}$, $\bar{p}_{eo}$ and $\bar{p}_{go}$. The system is obviously non-linear. Iterative method is used in obtaining the solution. Numerical computation has been programmed on a computer. Knowing $\bar{p}_{Fo}$, $\bar{p}_{Eo}$ and $\bar{p}_{Ro}$, the steady-state pressure distribution is explicitly given by (2.47) and (2.48).

Perturbation Solution

The perturbation pressure is governed by Eqs. (2.45b) and (2.46b) with one obvious boundary condition that $\bar{p}_1$ must vanish at $\xi = 0$ ($\bar{r} = 1$). The other boundary conditions are to be derived from the mass conservation and so on as follows:

First of all, since $\bar{p}_1$ is in general complex, it is convenient to assume

$$\bar{p}_o \bar{p}_1 = u(\xi) + i\, v(\xi) \tag{2.57}$$

Then, after separating the real and imaginary parts, the differential equations are reduced to

$$\left.\begin{aligned} \frac{d^2u}{d\xi^2} &= \frac{\sigma}{(1+\bar{h}_R)^3} e^{2\xi} \left[\frac{-(1+\bar{h}_R)\, v}{\bar{p}_o}\right] \\ \frac{d^2v}{d\xi^2} &= \frac{\sigma}{(1+\bar{h}_R)^3} e^{2\xi} \left[\bar{p}_o + \frac{1+\bar{h}_R}{\bar{p}_o}\, u\right] \end{aligned}\right\} \xi_F < \xi < \xi_R. \tag{2.58}$$

$$\left.\begin{aligned} \frac{d^2u}{d\xi^2} &= \sigma e^{2\xi} \left[-\frac{v}{\bar{p}_o} \right] \\ \frac{d^2v}{d\xi^2} &= \sigma e^{2\xi} \left[\bar{p}_o + \frac{u}{\bar{p}_o} \right] \end{aligned} \right\} \quad \xi_{R+} < \xi < o \tag{2.59}$$

Before Eqs. (2.34) and (2.36) can be used as boundary conditions for the differential equations, it is necessary to obtain expressions for $\bar{p}_{e1}$ and $\bar{p}_{g1}$.

Since p_e and f_e are functions of M_e we can write

$$p_e' = \frac{dp_e}{dM_e} M_e' \quad \text{and} \quad f_e' = \frac{df_e}{dM_e} M_e' \tag{2.60}$$

The primed quantities represent perturbations.

Also, from Eq. (2.18)

$$f_e = f_e (\dot{m}_F, a_e) \tag{2.61}$$

Thus,

$$\begin{aligned} f_e' &= \frac{\partial f_e}{\partial \dot{m}_F} \dot{m}_F' + \frac{\partial f_e}{\partial a_e} a_e' \\ &= \frac{f_e}{\dot{m}_{Fo}} \dot{m}_F' - \frac{f_e}{a_e} a_e' \end{aligned} \tag{2.62}$$

Combining (2.60) and (2.62)

$$\bar{p}_{e1} = \frac{d\bar{p}_e}{dM_e} \frac{f_e}{\frac{df_e}{dM_e}} \left[\frac{\dot{m}_{F1}}{\dot{m}_{Fo}} - \frac{1}{1 + \bar{h}_R} \right] \tag{2.63}$$

Similarly one can easily obtain

$$\bar{p}_{g1} = \frac{d\bar{p}_g}{dM_g} \frac{f_g}{\frac{df_g}{dM_g}} \left[\frac{\dot{m}_{R1}}{\dot{m}_{Ro}} - 1 - \frac{\bar{p}_{E1}}{\bar{p}_{Eo}} \right] \tag{2.64}$$

Using (2.63), (2.64), (2.30) and (2.32), Eqs. (2.34) and (2.36) become

$$- \frac{1}{\bar{P}_{Fo}\,(\bar{P}_s - \bar{P}_{Fo})}\,(u + iv)\Big|_{\xi_F} = \left(1 - \frac{H_e}{P_s - P_{eo}}\right)\left[2E^{-1}\,\frac{\partial(u + iv)}{\partial\xi}\right]_{\xi_F}$$

$$+ \frac{3}{1 + \bar{h}_R} - \frac{2H_e}{(\bar{P}_s - \bar{P}_{eo})(1 + \bar{h}_R)} \qquad (2.65)$$

$$\left[\frac{1}{\bar{P}_{Eo}}\left(\frac{1}{\bar{P}_{Eo} - \bar{P}_{Ro}}\right) - \frac{1}{\bar{P}_{Eo} - \bar{P}_{go}} - \frac{H_g}{\bar{P}_{Eo} - \bar{P}_{go}}\,\frac{1}{\bar{P}_{Eo}^{\,2}}\right](u + iv)\Big|_{\xi_{R-}}$$

$$= \frac{1}{\bar{P}_{Ro}(\bar{P}_{Eo} - \bar{P}_{Ro})}\,(u + iv)\Big|_{\xi_{R+}} + 2\left(1 - \frac{H_g}{\bar{P}_{Eo} - \bar{P}_{go}}\right)\left[E^{-1}\frac{\partial(u + iv)}{\partial\xi}\right]_{\xi_{R+}}$$

$$+ 3 - 2\,\frac{H_g}{\bar{P}_{Eo} - \bar{P}_{go}} \qquad (2.66)$$

where

$$\left.\begin{aligned} H_e &= \frac{d\bar{P}_e}{dM_e}\;f_e \Big/ \frac{df_e}{dM_e} \\ H_g &= \frac{d\bar{P}_g}{dM_g}\;f_g \Big/ \frac{df_g}{dM_g} \\ E &= \frac{d\bar{P}_o^{\,2}}{d\xi} \end{aligned}\right\} \qquad (2.67)$$

H_e and H_g can be determined by the relationships for an isentropic expansion or by simply using a gas table (Ref. 10).

The mass conservation at ξ_R yields

$$\frac{3}{1+\bar{h}_R} + 2\left[E^{-1}\ \frac{\partial(u+iv)}{\partial\xi}\right]_{\xi_{R-}} = 3 + 2\left[E^{-1}\ \frac{\partial(u+iv)}{\partial\xi}\right]_{\xi_{R+}} \tag{2.68}$$

Since the pressure at the exit of the film remains ambient in spite of the gap oscillation, the perturbation pressure must vanish.

$$(u+iv)\Big|_{\xi=0} = 0 \tag{2.69}$$

Each of the four equations, (2.65), (2.66), (2.68), and (2.69), yields two boundary conditions if their real and imaginary parts are separated. We therefore have eight boundary conditions to solve Eqs. (2.58) and (2.59).

The formulation of the perturbation problem is now complete. The numerical solution of this system is obtained in Appendix A using the matrix multiplication method.

An alternative approach using the nozzle equation instead of Vohr's correlation formula is given in Appendix B.

3. LOAD CAPACITY AND DYNAMIC BEARING REACTIONS

The pressure in the feeding hole region ($r<r_F$) is uniform and steady while the pressure distributions in the recessed pocket and in the film are given by

$$\bar{p}\,(\bar{r},\tau) = \bar{p}_o\,(\bar{r}) + \bar{\epsilon}\,\frac{u + i\,v}{\bar{p}_o}\,e^{i\tau}$$

$$= \bar{p}_o\,(\bar{r}) + \bar{\epsilon}\,\frac{u\,(\bar{r})\cos\tau - v\,(\bar{r})\sin\tau}{\bar{p}_o\,(\bar{r})} \qquad (3.1)$$

The bearing force may be obtained by integrating the pressure relative to the ambient, throughout the film. Thus,

$$W = \int_0^R (p - p_a)\;2\pi\,r\,d\,r$$

$$= \pi\,r_F^2\,(p_s - p_a) + 2\pi\int_{r_F}^{r_R}(p - p_a)\;r\,d\,r + 2\pi\int_{r_R}^{R}(p - p_a)\;r\,d\,r \qquad (3.2)$$

Non-dimensionalizing the load by $\pi R^2 p_a$, we have

$$\bar{W} = \frac{W}{\pi R^2 p_a} = \bar{r}_F^{\,2}\,(\bar{p}_s - 1) + 2\int_{\bar{r}_F}^{\bar{r}_R}(\bar{p}_o - 1 + \bar{\epsilon}\,\bar{p}_1\,e^{i\tau})\,\bar{r}\,d\,\bar{r}$$

$$+ 2\int_{\bar{r}_R}^{1}(\bar{p}_o - 1 + \bar{\epsilon}\,\bar{p}_1\,e^{i\tau})\,\bar{r}\,d\,\bar{r} \qquad (3.3)$$

Steady-State Load Capacity and Stiffness

The steady-state load capacity can be obtained by taking the time-independt part of Eq. (3.3).

$$\bar{W}_o = \bar{r}_F^{\,2}\,\bar{p}_s - 1 + 2\int_{\xi_F}^{\xi_R}\bar{p}_o\,(\xi)\;e^{2\xi}\;d\xi$$

$$+ 2\int_{\xi_R}^{o}\bar{p}_o\,(\xi)\;e^{2\xi}\;d\xi \qquad (3.4)$$

With the steady-state pressure distribution $\bar{p}_o(\bar{\xi})$ solved in the previous section, $\bar{W}_o$ can be easily obtained by quadrature. The static stiffness is, by definition,

$$\frac{Ck_o}{\pi R^2 p_a} = - C \frac{\partial}{\partial C}(\bar{W}_o) = - \frac{C}{2\Delta C}\left\{\bar{W}_o^{(+)} - \bar{W}_o^{(-)}\right\} \tag{3.5}$$

where the superscripts (+) and (-) refer to the load capacities at $C + \Delta C$ and $C - \Delta C$ respectively. ΔC should be sufficiently small; a suitable value for ΔC is $0.01C$.

Dynamic Bearing Reaction

The dynamic bearing reaction due to axial vibration is, from the time-dependent part of Eq. (3.3)

$$\frac{F_z}{\pi R^2 p_a} = \bar{\epsilon}\, 2 \int_{\bar{r}_F}^{1} \bar{p}_1\, \bar{r}\, d\bar{r}\, e^{i\tau}$$

$$= - \bar{\epsilon}\, R_e \left\{ e^{i\tau} (U_z + i\, V_z) \right\} \tag{3.6}$$

where U_z = Dynamic Stiffness

$$= - 2 \int_{\bar{\xi}_F}^{\bar{\xi}_R} \frac{u}{\bar{p}_o} e^{2\bar{\xi}}\, d\bar{\xi} - 2 \int_{\bar{\xi}_R}^{0} \frac{u}{\bar{p}_o} e^{2\bar{\xi}}\, d\bar{\xi} \tag{3.7}$$

V_z = Dynamic Damping

$$= - 2 \int_{\bar{\xi}_F}^{\bar{\xi}_R} \frac{v}{\bar{p}_o} e^{2\bar{\xi}}\, d\bar{\xi} - 2 \int_{\bar{\xi}_R}^{0} \frac{v}{\bar{p}_o} e^{2\bar{\xi}}\, d\bar{\xi} \tag{3.8}$$

Knowing u and v from the perturbation solution shown in the previous section, the dynamic stiffness and damping can be readily calculated from Eqs. (3.7) and (3.8) by quadrature.

Numerical computations have been programmed on a computer. Typical results are obtained for a bearing configuration with the following dimensions:

$$R = 2 \text{ in.}$$
$$r_R = 0.5 \text{ in.}$$
$$r_F = 0.005 \text{ in.}$$
$$h_R = 0.002 \text{ in.}$$

The static stiffness is plotted against Λ_s^* in Figs. 3 and 4 for $\bar{p}_s = 4$ and 2. It is seen that the static stiffness using Vohr's correlation has a maximum at approximately $\Lambda_s^* = 0.62$ for $\bar{p}_s = 4$ and $\Lambda_s^* = 0.50$ for $\bar{p}_s = 2$. The static stiffness using nozzle equation are also plotted for comparison; two different values of the flow discharge coefficient are used, namely, $C_w = 0.6$ and 1.0. Since Λ_s^* represents the relative importance of the restrictions offered by the restrictor and the bearing film, the peaks of the static stiffness occurs at different Λ_s^* for $C_w = 0.6$ and 1.0. The flow discharge coefficient for nozzles and orifices was reviewed in Ref. 11. It is reported that C_w varies from 0.6 to 1.0 depending on flow condition and pressure ratio. In general C_w is close to 1.0 when the pressure drop across the restrictor is large; this occurs when Λ_s^* is small (large clearance operation). When Λ_s^* is large (small clearance and hence no appreciable pressure drop across the restrictor), C_w is about 0.6. Although no measurement on C_w has been made for the inherently compensated restrictor used in this bearing, it is commonly accepted to use values between 0.6 and 1.0. For the bearing configuration under consideration the value of $C_w = 1.0$ appears to be a good choice as the static stiffness agrees well with that using Vohr's correlation.

Normally, a hydrostatic thrust bearing is designed off the optimum stiffness

point and on the larger Λ_s^* side for more stable operation (See Fig.10) and higher load capacity. It has been observed (Ref.13) that in a hydrostatic journal bearing, the actual stiffness on the high Λ_s^* side is appreciably below the theoretical value (using the nozzle equation and $C_w = 0.6$). The same type of comparison can be expected for hydrostatic thrust bearings. Thus, the present analysis using Vohr's correlation would yield results in better agreement with the actual stiffness.

The stiffness and load capacity for the same bearing except with a larger feeding hole ($r_F = 0.02$ in. instead of 0.005 in.), are shown in Figs. 5 and 6. The stiffness curves exhibit the same characteristics as the other bearing configuration; it again has a maximum stiffness at $\Lambda_s^* = 0.60$ if Vohr's correlation is used.

The dynamic stiffness and damping of the bearing with $r_F = 0.005$ in. are plotted against frequency for various values of C in Figs. 7 and 8. When the frequency is low ($\omega \lessapprox 1$), the dynamic stiffness approaches asymptotically to the value of the static stiffness as can be anticipated. The frequency at which $V_z = 0$, is called the critical frequency which will be useful in the stability analysis in the next section.

4. STABILITY

In the previous section, we have calculated the dynamic bearing reactions corresponding to small axial vibrations about the equilibrium (statically) position. These information are directly useful in determining the bearing stability.

In Reference 6, a stability analysis for either a single or two degree-of-freedom system was performed. The results for a single degree-of-freedom system are directly applicable; they may be stated as follows:

Let ω_o be the frequency of vibration at which

$$V_z\Big|_{\omega_o} = 0 \tag{4.1}$$

This is the state of neutral stability. Then, the critical mass is given by

$$M_o = \frac{P_a \pi R^2}{C\omega_o^2} U_z\Big|_{\omega_o} \tag{4.2}$$

A slight variation from the state of neutral stability would cause the system to be unstable if and only if

$$\frac{\partial V_z}{\partial \omega}\Big|_{\omega_o} \delta M > 0 \tag{4.3}$$

where δM is a small mass increment above M_o. From Figure 8, $\frac{\partial V_z}{\partial \omega}\Big|_{\omega_o} > 0$. Therefore, in order for the bearing to be stable, δM must be less than zero, or, the bearing mass must be kept below the critical mass.

Based on the above and a knowledge of U_z and V_z, the critical mass can be calculated from Eq. (4.2). Since Vohr's data (Ref. 4) are essentially for low Mach number flows, only bearings with subsonic flow throughout the passage will

be considered. Supersonic bearings are also currently under investigation.

The critical mass for the bearing with R = 2 in., r_R = 0.5 in., r_F = 0.005 in. and h_R = 0.002 in. is plotted against Λ_s^* in Fig. 9 for both methods of calculating restrictor flow. Although the critical mass calculated with C_w = 1.0 still appears to be in closer agreement with that according to Vohr's correlation, its error is not on the conservative side. In Fig. 10, the stiffness and the critical mass using Vohr's correlation are plotted against Λ_s^*. At the point where the stiffness is a maximum, the critical mass is rather low. A trade-off is therefore necessary between the stiffness and the critical mass. Figure 10 then would enable one to decide the design point of a bearing at which a stable operation is possible at the expense of a reasonable decrease in stiffness

It can also be seen from Fig. 10 that when Λ_s^* is beyond a certain value for a given $\bar{P}_s$, the bearing becomes infinitely stable because V_z is always positive there. Thus, we can obtain a stability map by plotting this critical Λ_s^* against $\bar{P}_s$ as shown in Fig. 11. Three curves are shown there; the solid one uses Vohr's correlation and the dotted curves use the nozzle formula. Again, the curve with C_w = 1.0 is not conservative. In Fig. 12, stability maps for different values of the pocket-to-film volume ratio are shown. It is seen that the bearing will be more stable for smaller pocket-to-film volume ratio. One can read from Fig. 12 for $\bar{P}_s$ = 4 for example, the values of critical Λ_s^* at different volume ratio.

$\frac{\pi r_R^2 h_R}{\pi(R^2 - r_R^2)C}$	$\frac{2}{3}$	$\frac{1}{3}$	$\frac{2}{15}$	$\frac{1}{15}$
Critical Λ_s^*	2.4	1.6	0.9	0.44

The dimensionless stiffness and the critical Λ_s^* are plotted against the volume ratio in Fig. 13. Note that we did not show the results with zero volume ratio; the reason was that the flow is choked and supersonic flow in the bearing film would result. From Fig. 13 it is clear that for the geometry chosen there is an optimum volume ratio of approximately 0.1 for maximum dimensionless static stiffness. It should be remarked here that one can design to achieve this stiffness with the assurance that the bearing with Λ_s^* = 0.7 (which is the critical value) and volume ratio of 0.1, is at the threshold of absolute stability.

5. SUMMARY AND CONCLUSIONS

Inherently compensated hydrostatic bearings with shallow recessed pocket near the feeding hole were analyzed theoretically. Both the bearing film and the recessed pocket are treated by using the isothermal Reynolds' equation. Vohr's correlation for entrance restriction was used to calculate the restrictor flow. Results were compared with those using the nozzle formula instead.

Based on the results obtained, the following conclusions can be drawn:

1. Steady-state load capacity and stiffness were calculated. It was found that the static stiffness has a maximum value when the feeding parameter Λ_s^* is approximately 0.6 for the geometry chosen if Vohr's correlation is used.

2. If the nozzle formula is used to calculate the restrictor flow, then the discharge coefficient $C_w = 1.0$ yields good results in static stiffness but non-conservative stability margin.

3. Stability results were obtained based on a perturbation analysis which yields dynamic stiffness and dynamic damping. Applying the stability results of Ref. 6, stability maps were constructed. A combined plot of stiffness and critical mass against the feeding parameter shows that it is often necessary to design a bearing off its maximum stiffness in order to gain a sufficient stability margin.

4. The stability margin of a hydrostatic bearing increases with decreasing volume ratio between the recessed pocket and the bearing film.

5. If a hydrostatic bearing is designed at the threshold of absolute stability, there is an optimum pocket-to-film volume ratio at which the static stiffness is a maximum.

NOMENCLATURE

A_e	Area = $2\pi r_F (C + h_R)$
C	Equilibrium film thickness; Also speed of sound
C*	Speed of sound at sonic speed
C_w	Nozzle discharge coefficient
E	Defined in (2.67)
$\bar{f}(\eta)$	Defined in (B.3)
f_e, f_g	Defined in (2.18), (2.22)
F_z	Dynamic bearing reaction
H_e, H_g	Defined in (2.67)
$[\bar{H}]$	Matrix defined in (A.20)
h	Film thickness
h_R	Depth of recessed pocket
$\bar{h}$	h/C, dimensionless film thickness
i	$\sqrt{-1}$
k_o	Static bearing stiffness
K'	$K \bar{R}_e$

K	Constant defined in (2.11)
M	Mass of bearing
M_e	Mach number
M_e^*	Mach number based on C*
$\dot{m}$	Mass flow rate
$\dot{m}_o$	Steady-state mass flow rate
$\bar{\dot{m}}$	Dimensionless mass flow rate, Eq. (2.51)
p	Pressure
p_a	Ambient pressure
p_{dyn}	Dynamic pressure head
p_e	Defined in (2.13)
p_g	Defined in (2.21)
p_s	Supply pressure
$\bar{p}$	p/p_a
$\bar{p}_o$, $\bar{p}_1$	Steady-state and perturbation pressure, defined in (2.24)
r	Radial coordinate
$\bar{r}$	r/R

r_F	Radius of feeding hole
r_R	Radius of recessed pocket
R	Bearing radius
$\bar{R}_e$	Reynold's number = $\dot{m}/(\pi\, r\, \mu)$
$\mathcal{R}$	Gas constant
T	Temperature
t	Time
U_z	Dimensionless dynamic stiffness
V_z	Dimensionless dynamic damping
u, v	Defined in (2.57)
V	Gas velocity
W	Bearing load capacity
$\bar{W}$	$W/\pi R^2 p_a$
γ	Ratio of specific heats
ϵ	Amplitude of axial vibration
$\bar{\epsilon}$	Dimensionless ϵ, $\bar{\epsilon} = \epsilon/C$
Λ_s^*	Feeding parameter, defined in (2.52)

μ Viscosity

ξ $\ell n\ \bar{r}$

ρ Density

σ Squeeze number, defined in (2.6)

τ Dimensionless time, ωt

ω Frequency of vibration

ω_o Critical ω

Subscript

o, 1 Steady-state and perturbation quantities

F,E,R Pertaining to geometrical location, see Fig. 1

Superscripts

$-$ Denotes dimensionless quantities

k Indicates station

REFERENCES

1. Licht, L., Fuller, D.D., and Sternlicht, B., "Self-Excited Vibration of an Air-Lubricated Thrust Bearing," Trans. ASME, vol. 80, p.411, 1958.

2. Licht, L., and Elrod, H.G., Jr., "An Analytical and Experimental Study of the Stability of Externally Pressurized, Gas-Lubricated Thrust Bearings," The Franklin Institute, Report No. 1-A2049-12, 1961.

3. Lund, J., Wernick, R.J., and Malanoski, S.B., "Analysis of the Hydrostatic Journal and Thrust Gas Bearing for the NASA AB-5 Gyro Gimbal Bearing," MTI Technical Report 62TR26, 1962.

4. Vohr, J., "An Experimental Study of Flow Phenomena in the Feeding Region of an Externally Pressurized Gas Bearing," MTI Technical Report 65TR47, 1966.

5. Carfagno, S.P., and McCabe, J.T., "Summary of Investigations of Entrance Effects in Circular Thrust Bearings," Franklin Institute Research Laboratories Interim Report 1-A2049, 1965.

6. Pan, C.H.T., "Spectral Analysis of Gas Bearing Systems for Stability Studies," presented at the Ninth Midwestern Mechanics Conference, University of Wisconsin, Madison, Wis., August, 1965.

7. Ralston, A., and Wilf, H.S., "Mathematical Methods for Digital Computers," John Wiley & Sons, Inc., New York, N.Y., 1960.

8. Castelli, V., and Pirvics, J., "Equilibrium Characteristics of Axial-Groove Gas Lubricated Bearings," ASLE-ASME-ASLE Lubrication Conference, San Francisco, California, October, 1965.

9. Hildebrand, F.B., "Introduction to Numerical Analysis," McGraw-Hill Co., New York, N.Y., 1956.

10. Keenan, J.H. and Kaye, J. "Gas Tables" John Wiley & Sons, Inc., 1956.

11. Hsing, F.C. and Chiang, T., "A Review of the Discharge Coefficient of Orifices and Nozzles," MTI-65-TM7, October, 1965.

12. Chiang, T., and Pan, C.H.T., "Analysis of Pneumatic Hammer Instability of Inherently Compensated Hydrostatic Thrust Gas Bearings" MTI-66TR47, January 1967.

13. Wilson, D., Private Communication on his unpublished experimental data.

APPENDIX A THE MATRIX MULTIPLICATION METHOD IN SOLVING ORDINARY DIFFERENTIAL EQUATIONS

The differential equations (2.58) and (2.59) derived in Section 2 are to be solved by using the matrix multiplication method. Rewrite the equation in the following form.

$$\left.\begin{aligned} u'' + f_1 v &= f_2 \\ v'' + g_1 u &= g_2 \end{aligned}\right] \qquad \xi_F < \xi < \xi_{R-} \tag{A.1}$$

$$\left.\begin{aligned} u'' + \bar{f}_1 v &= \bar{f}_2 \\ v'' + \bar{g}_1 u &= \bar{g}_2 \end{aligned}\right] \qquad \xi_{R+} < \xi < 0 \tag{A.2}$$

where

$$\left.\begin{aligned} f_1 &= \frac{\sigma}{(1+\bar{h}_R)^2}\,\frac{e^{2\xi}}{\bar{p}_o} = -g_1 \\ f_2 &= 0 \\ g_2 &= \frac{\sigma}{(1+\bar{h}_R)^3}\, e^{2\xi}\,\bar{p}_o \\ \bar{f}_1 &= \sigma e^{2\xi}\,\bar{p}_o = -\bar{g}_1 \\ \bar{f}_2 &= 0 \\ g_2 &= \sigma e^{2\xi}\,\bar{p}_o \end{aligned}\right] \tag{A.3}$$

The primes represent derivations with respect to ξ. If we divide the distance between ξ_F and ξ_R into N equal intervals and the distance between ξ_R and 0 into Q intervals,

$$\left.\begin{aligned} \Delta_1 &= \frac{\xi_R - \xi_F}{N} \\ \Delta_2 &= \frac{0 - \xi_R}{Q} \end{aligned}\right] \tag{A.4}$$

then, in central difference form,

$$\left.\begin{aligned} u'(\xi_k) &= \frac{u^{k+1} - 2u^k + u^{k-1}}{\Delta_1} \\ u''(\xi_k) &= \frac{u^{k+1} - 2u^k + u^{k-1}}{\Delta_1^2} \end{aligned}\right\} \quad k = 0, 1, 2, \ldots N$$

$$\left.\begin{aligned} u'(\xi_k) &= \frac{u^{k+1} - 2u^k + u^{k-1}}{\Delta_2} \\ u''(\xi_k) &= \frac{u^{k+1} - 2u^k + u^{k-1}}{\Delta_2^2} \end{aligned}\right\} \quad k = N', N+1, \ldots N+Q$$

where $u^k = u(\xi_k)$. Note that stations N and N' occupy the same physical location.

Substitute into Eqs. (A.1) and (A.2) and write the results in matrix form

$$\left[A^k\right] y^{k+1} + \left[B^k\right] y^k + \left[C^k\right] y^{k-1} = d^k,$$

$$(k = 0, 1, 2, \ldots N) \qquad (A.5)$$

$$\left[\bar{A}^k\right] y^{k+1} + \left[\bar{B}^k\right] y^k + \left[\bar{C}^k\right] y^{k-1} = \bar{d}^k,$$

$$(k = N', N+1, \ldots N+Q) \qquad (A.6)$$

where

$$A^k = \frac{1}{\Delta_1^2}\left[I\right] = \frac{1}{\Delta_1^2}\begin{bmatrix} 1 & 0 \\ 0 & 1 \end{bmatrix}$$

$$B^k = \begin{bmatrix} \frac{-2}{\Delta_1^2} & f_1^k \\ g_1^k & \frac{-2}{\Delta_1^2} \end{bmatrix}$$

$$C^k = A^k$$

$$d^k = \begin{bmatrix} f_2^k \\ g_2^k \end{bmatrix} \quad ; \quad y^k = \begin{bmatrix} u^k \\ v^k \end{bmatrix}$$

$$\bar{A}^k = \frac{1}{\Delta_1^2} \begin{bmatrix} I \end{bmatrix}$$

$$\bar{B}^k = \begin{bmatrix} \frac{-2}{\Delta_2^2} & \bar{f}_1^k \\ \bar{g}_1^k & \frac{-2}{\Delta_2^2} \end{bmatrix}$$

$$\bar{C}^k = \bar{A}^k$$

$$\bar{d}^k = \begin{bmatrix} \bar{f}_2^k \\ \bar{g}_2^k \end{bmatrix}$$

Assume that the y-vector at station "k+1" can be expressed by

$$y^{k+1} = M^k y^k + m^k \qquad (A.7)$$

Here, M^k and m^k are unknown matrix and vector at station "k". Combining (A.6) and (A.7) we obtain

$$\left.\begin{aligned} M^{k-1} &= \left[\bar{A}^k M^k + \bar{B}^k\right]^{-1} \left[-\bar{C}^k\right] \\ m^{k-1} &= \left[\bar{A}^k M^k + \bar{B}^k\right]^{-1} \left(\bar{d}^k - \bar{A}^k m^k\right) \end{aligned}\right\} \quad k = N', N+1, \ldots N+Q \qquad (A.8)$$

From boundary condition (2.69) it is obvious that

$$y^{N+Q} = \begin{bmatrix} 0 \\ 0 \end{bmatrix} \qquad (A.9)$$

Using (A.7) and setting $k = N + Q - 1$,

$$y^{N+Q} = M^{N+Q-1}\, y^{N+Q-1} + m^{N+Q-1} \tag{A.10}$$

Since y^{N+Q-1} is not equal to zero, in order to satisfy (A.9) we must have

$$\begin{aligned} M^{N+Q-1} &= 0 \\ m^{N+Q-1} &= 0 \end{aligned} \tag{A.11}$$

Using (A.8) as the recursion formula, the following is easily obtained.

$$\left.\begin{aligned}
M^{N+Q-2} &= \left[\bar{A}^{N+Q-1}\, M^{N+Q-1} + \bar{B}^{N+Q-1}\right]^{-1} \left[-\bar{C}^{N+Q-1}\right] \\
m^{N+Q-2} &= \left[\bar{A}^{N+Q-1}\, M^{N+Q-1} + \bar{B}^{N+Q-1}\right]^{-1} \left(\bar{d}^{N+Q-1} - \bar{A}^{N+Q-1}\, m^{N+Q-1}\right) \\
M^{N+Q-3} &= \left[\bar{A}^{N+Q-2}\, M^{N+Q-2} + \bar{B}^{N+Q-2}\right]^{-1} \left[-\bar{C}^{N+Q-2}\right] \\
m^{N+Q-3} &= \left[\bar{A}^{N+Q-2}\, M^{N+Q-2} + \bar{B}^{N+Q-2}\right]^{-1} \left(\bar{d}^{N+Q-2} - \bar{A}^{N+Q-2}\, m^{N+Q-2}\right) \\
&\text{- -} \\
M^{N'} &= \left[\bar{A}^{N+1}\, M^{N+1} + \bar{B}^{N+1}\right]^{-1} \left[-\bar{C}^{N+1}\right] \\
m^{N'} &= \left[\bar{A}^{N+1}\, M^{N+1} + \bar{B}^{N+1}\right]^{-1} \left(\bar{d}^{N+1} - \bar{A}^{N+1}\, m^{N+1}\right)
\end{aligned}\right] \tag{A.12}$$

Define

$$\left.\begin{aligned}
\alpha_1 &= \frac{1}{\bar{P}_{Eo}} \left(\bar{P}_{Ro} - \bar{P}_{go}\right) - H_g \frac{\bar{P}_{Eo} - \bar{P}_{Ro}}{\bar{P}_{Eo}^{\,2}} \\
\alpha_2 &= \left(\bar{P}_{Eo} - \bar{P}_{go}\right) \Big/ \bar{P}_{Ro} \\
\alpha_3 &= 2\xi_R \left(\bar{P}_{Eo} - \bar{P}_{go} - H_g\right) \left(\bar{P}_{Eo} - \bar{P}_{Ro}\right) \Big/ \left(\bar{P}_{Ro}^{\,2} - 1\right) \\
\alpha_4 &= \left[3\left(\bar{P}_{Eo} - \bar{P}_{go}\right) - 2H_g\right] \left(\bar{P}_{Eo} - \bar{P}_{Ro}\right)
\end{aligned}\right] \tag{A.13}$$

Then, Eq. (2.66) takes the form,

$$\alpha_1 \, (u + iv)\Big|_{\xi_{R-}} = \alpha_2 \, (u + iv)\Big|_{\xi_{R+}} + \alpha_3 \, \frac{\partial \, (u + iv)}{\partial \xi}\Big|_{\xi_{R+}} + \alpha_4$$

or,

$$\alpha_1 \, y^N = \alpha_2 \, y^{N'} + \frac{\alpha_3}{\Delta_2} \left(- \frac{1}{2} \, y^{N+2} + 2y^{N+1} - \frac{3}{2} \, y^{N'} \right) + C_4 \qquad \text{(A.14)}$$

where $C_4 = \begin{bmatrix} \alpha_4 \\ o \end{bmatrix}$. We have used the forward difference formula.

From (A.7), one can write

$$y^{N+2} = M^{N+1} \, y^{N+1} + m^{N+1}$$

$$y^{N+1} = M^{N'} \, y^{N'} + m^{N'}$$

Substituting into (A.14) results in

$$\alpha_1 \, y^N = \left[G \right] y^{N'} + g \qquad \text{(A.15)}$$

where

$$\left.\begin{aligned} \left[G \right] &= \left[\left(\alpha_2 - \frac{3}{2} \, \frac{\alpha_3}{\Delta_2} \right) I \right] + \frac{\alpha_3}{\Delta_2} \left[- \frac{1}{2} \, M^{N+1} + 2I \right] \left[M^{N'} \right] \\ \left[g \right] &= - \frac{1}{2} \, \frac{\alpha_3}{\Delta_2} \, m^{N+1} + \frac{\alpha_3}{\Delta_2} \left[- \frac{1}{2} \, M^{N+1} + 2I \right] m^{N'} + C_4 \end{aligned}\right\} \qquad \text{(A.16)}$$

From (2.68) we have

$$\frac{\partial \, (u + iv)}{\partial \xi}\Big|_{\xi_{R-}} = \alpha_5 \, \frac{\partial \, (u + iv)}{\partial \xi}\Big|_{\xi_{R+}} + \alpha_6 \qquad \text{(A.17)}$$

where

$$\alpha_5 = \frac{\bar{P}_{Fo}^2 - \bar{P}_{Eo}^2}{\xi_F - \xi_R} \quad \frac{\xi_R}{\bar{P}_{Ro}^2 - 1}$$

$$\alpha_6 = \frac{\bar{P}_{Fo}^2 - \bar{P}_{Eo}^2}{\xi_F - \xi_R} \quad \frac{3}{2} \quad \frac{\bar{h}_R}{1 + \bar{h}_R} \qquad \text{(A.18)}$$

Thus,

$$\left[\frac{3}{2}\ y^N - 2\ y^{N-1} + \frac{1}{2}\ y^{N-2}\right] = \frac{\Delta_1\ \alpha_5}{\Delta_2}\left[-\frac{1}{2}\ y^{N+2} + 2y^{N+1} - \frac{3}{2}\ y^{N'}\right] + \left[\begin{matrix}\Delta_1\ \alpha_6 \\ 0\end{matrix}\right]$$

Using (A.5) to eliminate y^{N-2}, and (A.7) to eliminate y^{N+2} and y^{N+1}, we obtain

$$\left[\frac{3}{2}\ I - \frac{1}{2}\left[C^{N-1}\right]^{-1}\left[A^{N-1}\right]\right] y^N + \left[-2I - \frac{1}{2}\left[C^{N-1}\right]^{-1}\left[B^{N-1}\right]\right] y^{N-1} + \frac{1}{2}\left[C^{N-1}\right]^{-1} d^{N-1}$$

$$= \frac{\Delta_1}{\Delta_2}\ \alpha_5\left\{\left[\bar{H}\right] y^{N'} + \left[-\frac{1}{2}\ M^{N+1} + 2I\right]\ m^{N'} - \frac{1}{2}\ m^{N+1}\right\} + C_6 \qquad \text{(A.19)}$$

where

$$\left[\bar{H}\right] = \left[-\frac{1}{2}\ M^{N+1} + 2I\right]\left[M^{N'}\right] - \frac{3}{2}\ I$$

$$C_6 = \left[\begin{matrix}\Delta_1\ \alpha_6 \\ 0\end{matrix}\right] \qquad \text{(A.20)}$$

Using (A.15) to eliminate $y^{N'}$ in (A.19),

$$\left[L\right] y^N = \left[2\ I + \frac{1}{2}\left[C^{N-1}\right]^{-1}\left[B^{N-1}\right]\right] y^{N-1} + \left\{-\frac{1}{2}\left[C^{N-1}\right]^{-1} d^{N-1} + C_6\right.$$

$$\left. + \frac{\Delta_1}{\Delta_2}\ \alpha_5\ (\bar{H}\ G^{-1}\ g + \left[-\frac{1}{2}\ M^{N+1} + 2\ I\right] m^{N'} - \frac{1}{2}\ m^{N+1})\right\} \qquad \text{(A.21)}$$

where

$$[L] = \frac{3}{2} I - \frac{1}{2}\left[C^{N-1}\right]^{-1}\left[A^{N-1}\right] - \frac{\Delta_1}{\Delta_2}\,\alpha_1\,\alpha_5\,\bar{H}\,G^{-1} \tag{A.22}$$

Thus, by comparing (A.7) with (A.21) it is clear that

$$M^{N-1} = 2[L]^{-1} + \frac{1}{2}[L]^{-1}\left[C^{N-1}\right]^{-1}\left[B^{N-1}\right] \tag{A.23}$$

$$m^{N-1} = -\frac{1}{2}[L]^{-1}\left[C^{N-1}\right]^{-1} d^{N-1} + [L]^{-1} c_6 + \frac{\Delta_1}{\Delta_2}\alpha_5\left([L]^{-1}[\bar{H}][G]^{-1} g + [L]^{-1}\left[-\frac{1}{2}M^{N+1} + 2I\right] m^{N'} - \frac{1}{2}[L]^{-1} m^{N+1}\right) \tag{A.24}$$

From which we can calculate the rest of the M's and m's.

$$\left.\begin{aligned} M^{N-2} &= \left[A^{N-1} M^{N-1} + B^{N-1}\right]^{-1}\left[-C^{N-1}\right] \\ m^{N-2} &= \left[A^{N-1} M^{N-1} + B^{N-1}\right]^{-1}\left[d^{N-1} - A^{N-1} m^{N-1}\right] \\ M^{N-3} &= \left[A^{N-2} M^{N-2} + B^{N-2}\right]^{-1}\left[-C^{N-2}\right] \\ m^{N-3} &= \left[A^{N-2} M^{N-2} + B^{N-2}\right]^{-1}\left[d^{N-2} - A^{N-2} m^{N-2}\right] \end{aligned}\right\} \tag{A.25}$$

Finally, from boundary condition (2.65),

$$-\frac{1}{\bar{p}_{Fo}(\bar{p}_s - \bar{p}_{Fo})} y^{(o)} = \left(1 - \frac{H_e/p_a}{\bar{p}_s - \bar{p}_{eo}}\right) 2\,\frac{\bar{\rho}_F - \bar{\rho}_R}{\bar{p}_{Fo}^2 - \bar{p}_{Lo}^2}\,\frac{1}{\Delta_1}\left(-\frac{1}{2} y^{(2)} + 2y^{(1)} - \frac{3}{2} y^{(o)}\right)$$

$$+ \frac{3}{1 + \bar{h}_R} - \frac{2\,H_e/p_a}{(\bar{p}_s - \bar{p}_{eo})(1 + \bar{h}_R)} \tag{A.26}$$

Define

$$\left.\begin{aligned} \alpha_7 &= \frac{1}{\bar{P}_{Fo}(\bar{P}_s - \bar{P}_{Fo})} \\ \alpha_8 &= \left(1 - \frac{H_e/p_a}{\bar{P}_s - \bar{P}_{eo}}\right) 2\, \frac{\bar{\rho}_F - \bar{\rho}_R}{\bar{P}_{Fo}^2 - \bar{P}_{Eo}^2} \\ \alpha_9 &= \frac{3}{1 + \bar{h}_R} - \frac{2\, H_e/p_a}{(\bar{P}_s - \bar{P}_{eo})(1 + \bar{h}_R)} \end{aligned}\right] \qquad (A.27)$$

Then, Eq. (A.26) becomes

$$\left[\left(\alpha_7 - \frac{3}{2}\,\frac{\alpha_8}{\Delta_1}\right) I - \frac{1}{2}\,\frac{\alpha_8}{\Delta_1}\, M^{(1)}\, M^{(o)} + 2\,\frac{\alpha_8}{\Delta_1}\, M^{(o)}\right] y^{(o)}$$

$$+ \frac{\alpha_8}{\Delta_1}\left[-\frac{1}{2} M^{(1)} + 2\, I\right] m^{(o)} - \frac{\alpha_8}{2\Delta_1}\, m^{(1)} + C_9 = 0 \qquad (A.28)$$

where

$$C_9 = \begin{bmatrix} \alpha_9 \\ 0 \end{bmatrix}$$

Thus,

$$y^{(o)} = -\left[\left(\alpha_7 - \frac{3}{2}\,\frac{\alpha_8}{\Delta_1}\right) I - \frac{1}{2}\,\frac{\alpha_8}{\Delta_1}\, M^{(1)}\, M^{(o)} + 2\,\frac{\alpha_8}{\Delta_1}\, M^{(o)}\right]^{-1} \cdot$$

$$\left(\frac{\alpha_8}{\Delta_1}\left[-\frac{1}{2} M^{(1)} + 2\, I\right] m^{(o)} - \frac{\alpha_8}{2\Delta_1}\, m^{(1)} + C_9\right) \qquad (A.29)$$

Knowing $y^{(o)}$ from (A.29) and M's and m's from (A.12) and (A.25), we can write down the solution as follows:

$$\left.\begin{aligned}
y^{(1)} &= M^{(o)}\, y^{(o)} + m^{(o)} \\
y^{(2)} &= M^{(1)}\, y^{(1)} + m^{(1)} \\
&\vdots \\
y^{N} &= M^{N-1}\, y^{N-1} + m^{N-1} \\
y^{N'} &= \alpha_1 [G]^{-1} y^{N} - [G]^{-1} g \\
y^{N+1} &= M^{N'}\, y^{N'} + m^{N'} \\
y^{N+2} &= M^{N+1}\, y^{N+1} + m^{N+1} \\
&\vdots \\
y^{N+Q} &= M^{N+Q-1}\, y^{N+Q-1} + m^{N+Q-1}
\end{aligned}\right\} \qquad \text{(A.30)}$$

APPENDIX B ALTERNATE METHOD USING THE NOZZLE EQUATION

Instead of using the Vohr's correlation formula, the well-known nozzle equation will be used to compute the flow and pressure drop through the restrictors. The mass flow rates at r_F and r_R are

$$\dot{m}_F = C_w \left[2\pi r_F (h + h_R)\right] \sqrt{\frac{2\gamma}{\gamma-1}} \quad \frac{p_s}{\sqrt{\mathcal{R}T}} \quad \bar{f} \left(\frac{p}{p_s}\right) \tag{B.1}$$

$$\dot{m}_R = C_w \left(2\pi r_R h\right) \sqrt{\frac{2\gamma}{\gamma-1}} \quad \frac{\rho_E}{\sqrt{\mathcal{R}T}} \quad \bar{f} \left(\frac{p}{p_E}\right) \tag{B.2}$$

where C_w = discharge coefficient

$$\bar{f}(\eta) \equiv \eta^{\frac{1}{\gamma}} \left[1 - \eta^{\frac{\gamma-1}{\gamma}}\right]^{1/2} \tag{B.3}$$

Nondimensionalize the mass flux by

$\rho_s \sqrt{\mathcal{R}T}\ 2\pi r_F\ (C + h_R)$ as before,

$$\bar{\dot{m}}_F = C_w \sqrt{\frac{2\gamma}{\gamma-1}} \left(1 + \frac{1}{1 + \bar{h}_R} \bar{\epsilon} e^{i\tau}\right) \bar{f} \left(\frac{p}{p_s}\right) \tag{B.4}$$

$$\bar{\dot{m}}_R = C_w \sqrt{\frac{2\gamma}{\gamma-1}} \quad \frac{1}{1 + \bar{h}_R} \left(1 + \bar{\epsilon} e^{i\tau}\right) \frac{r_R}{r_F} \frac{p_E}{p_s} \bar{f} \left(\frac{p}{p_E}\right) \tag{B.5}$$

Apply perturbation to (B.4) and (B.5)

$$\bar{\dot{m}}_{Fo} + \bar{\epsilon}\ \bar{\dot{m}}_{F1}\ e^{i\tau} = C_w \sqrt{\frac{2\gamma}{\gamma-1}} \left(1 + \frac{1}{1 + \bar{h}_R} \bar{\epsilon} e^{i\tau}\right) \left(\bar{f}\left|_{\frac{p_{Fo}}{p_s}} + \frac{d\bar{f}}{d\eta}\right|_{\frac{p_{Fo}}{p_s}} \bar{\epsilon} \frac{p_{F1}}{p_s} e^{i\tau}\right) \tag{B.6}$$

$$\bar{\dot{m}}_{Ro} + \bar{\epsilon}\ \bar{\dot{m}}_{R_1}\ e^{i\tau} = C_w \sqrt{\frac{2\gamma}{\gamma-1}}\ \frac{1 + \bar{\epsilon}\ e^{i\tau}}{1 + \bar{h}_R}\ \frac{r_R}{r_F}\ \frac{p_{Eo} + \bar{\epsilon}\ p_{E1}\ e^{i\tau}}{p_s}$$

$$\left\{ f \left|_{\frac{p_{Ro}}{p_{Eo}}} + \frac{d\bar{f}}{d\eta}\right|_{\frac{p_{Ro}}{p_{Eo}}} \left(\frac{1}{p_{Eo}}\ \bar{\epsilon}\ p_{R1}\ e^{i\tau} - \frac{p_{Ro}}{p_{Eo}^2}\ \bar{\epsilon}\ p_{E1}\ e^{i\tau} \right) \right\} \qquad (B.7)$$

Thus, we have

$$\bar{\dot{m}}_o = C_w \sqrt{\frac{2\gamma}{\gamma-1}}\ \bar{f}\left|_{\frac{\bar{p}_{Fo}}{\bar{p}_s}}\right. \qquad (B.8)$$

$$\bar{\dot{m}}_o = C_w \sqrt{\frac{2\gamma}{\gamma-1}}\ \frac{1}{1 + \bar{h}_R}\ \frac{\bar{r}_R}{\bar{r}_F}\ \frac{\bar{p}_{Fo}}{\bar{p}_s}\ \bar{f}\left|_{\frac{\bar{p}_{Ro}}{\bar{p}_{Eo}}}\right. \qquad (B.9)$$

Equations (B.8), (B.9), (2.49) and (2.50) can be solved for $\bar{\dot{m}}_o$, $\bar{p}_{Fo}$, $\bar{p}_{Eo}$ and $\bar{p}_{Ro}$. Hence, the steady-state pressure distribution is readily obtained by Eqs. (2.47) and (2.48).

The differential equations derived for the perturbation pressure are of course still applicable in this method. Equations (B.6) and (B.7) should be used to obtain boundary conditions to replace Eqs. (2.65) and (2.66)

From Eqs. (2.30) and (B.6), we obtain, after some manipulation,

$$\frac{1}{\bar{p}_s\ \bar{p}_{Fo}}\ (u + iv)\left|_{\xi_F}\right. = \frac{\bar{f}}{\frac{d\bar{f}}{d\eta}}\left|_{\frac{\bar{p}_{Fo}}{\bar{p}_s}}\right. \left\{ \frac{2}{1 + \bar{h}_R} + 2 \left[E^{-1}\ \frac{\partial(u + iv)}{\partial\xi} \right]_{\xi_F} \right\} \qquad (B.10)$$

Similarly, from Eqs. (2.32) and (B.7)

$$\left(\frac{1}{\bar{p}_{Eo}^{\,2}} - \frac{d\bar{f}/d\eta}{\bar{f}}\left|\begin{matrix}\bar{p}_{Ro}\\ \bar{p}_{Eo}\end{matrix}\right.\frac{\bar{p}_{Ro}}{\bar{p}_{Eo}^{\,3}}\right)(u+iv)\Bigg|_{\xi_{R-}} + \frac{d\bar{f}/d\eta}{\bar{f}}\left|\begin{matrix}\bar{p}_{Ro}\\ \bar{p}_{Eo}\end{matrix}\right.\frac{1}{\bar{p}_{Ro}\,\bar{p}_{Eo}}(u+iv)\Bigg|_{\xi_{R+}}$$

$$= 2 + 2\left[E^{-1}\,\frac{\partial(u+iv)}{\partial\xi}\right]_{\xi_{R+}} \qquad (B.11)$$

Comparing (B.10), (B.11) with (2.65), (2.66), it can be seen that if we define

$$\left.\begin{aligned}
\alpha_1' &= \frac{1}{\bar{p}_{Eo}^{\,2}} - \mathcal{G}\left|\begin{matrix}\bar{p}_{Ro}\\ \bar{p}_{Eo}\end{matrix}\right.\frac{\bar{p}_{Ro}}{\bar{p}_{Eo}^{\,3}}\\
\alpha_2' &= -\mathcal{G}\left|\begin{matrix}\bar{p}_{Ro}\\ \bar{p}_{Eo}\end{matrix}\right.\frac{1}{\bar{p}_{Ro}\,\bar{p}_{Eo}}\\
\alpha_3' &= \frac{2\xi_R}{\bar{p}_{Ro}^{\,2}-1}\\
\alpha_4' &= 2 \quad ; \quad \mathcal{G} \equiv \frac{d\bar{f}/d\eta}{\bar{f}}\\
\alpha_7' &= -\frac{1}{\bar{p}_s\,\bar{p}_{Fo}}\\
\alpha_8' &= \frac{1}{\mathcal{G}\left|\begin{matrix}\bar{p}_{Fo}\\ \bar{p}_s\end{matrix}\right.}\,2\,\frac{\xi_F-\xi_R}{\bar{p}_{Fo}^{\,2}-\bar{p}_{Eo}^{\,2}}\\
\alpha_9' &= \frac{1}{\mathcal{G}\left|\begin{matrix}\bar{p}_{Fo}\\ \bar{p}_s\end{matrix}\right.}\,\frac{2}{1+\bar{h}_R}
\end{aligned}\right\} \qquad (B.12)$$

the numerical scheme in Appendix A can be used for this alternative method utilizing the nozzle equation provided that α_1, α_2, etc. are replaced by the primed quantities defined in (B.12).

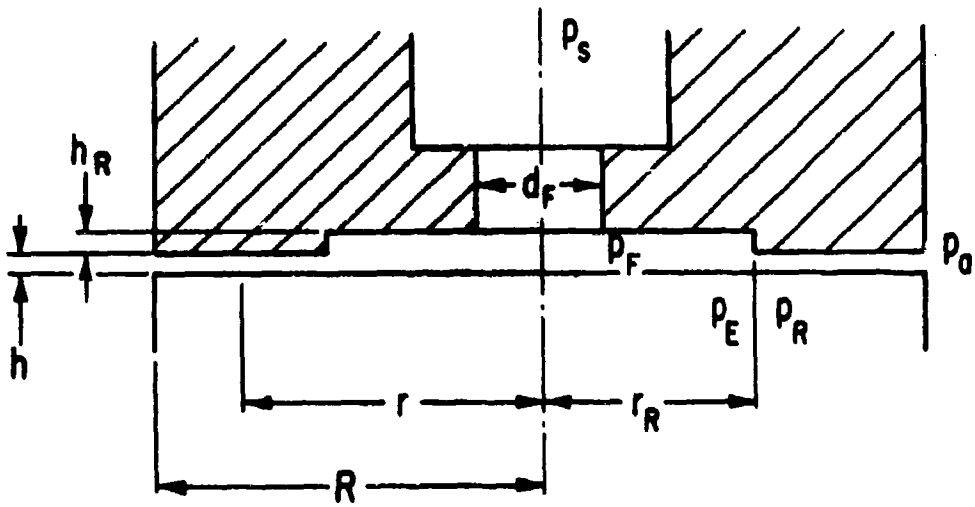

Fig. 1 Geometry of an Inherently Compensated, Hydrostatic, Circular, Thrust Bearing

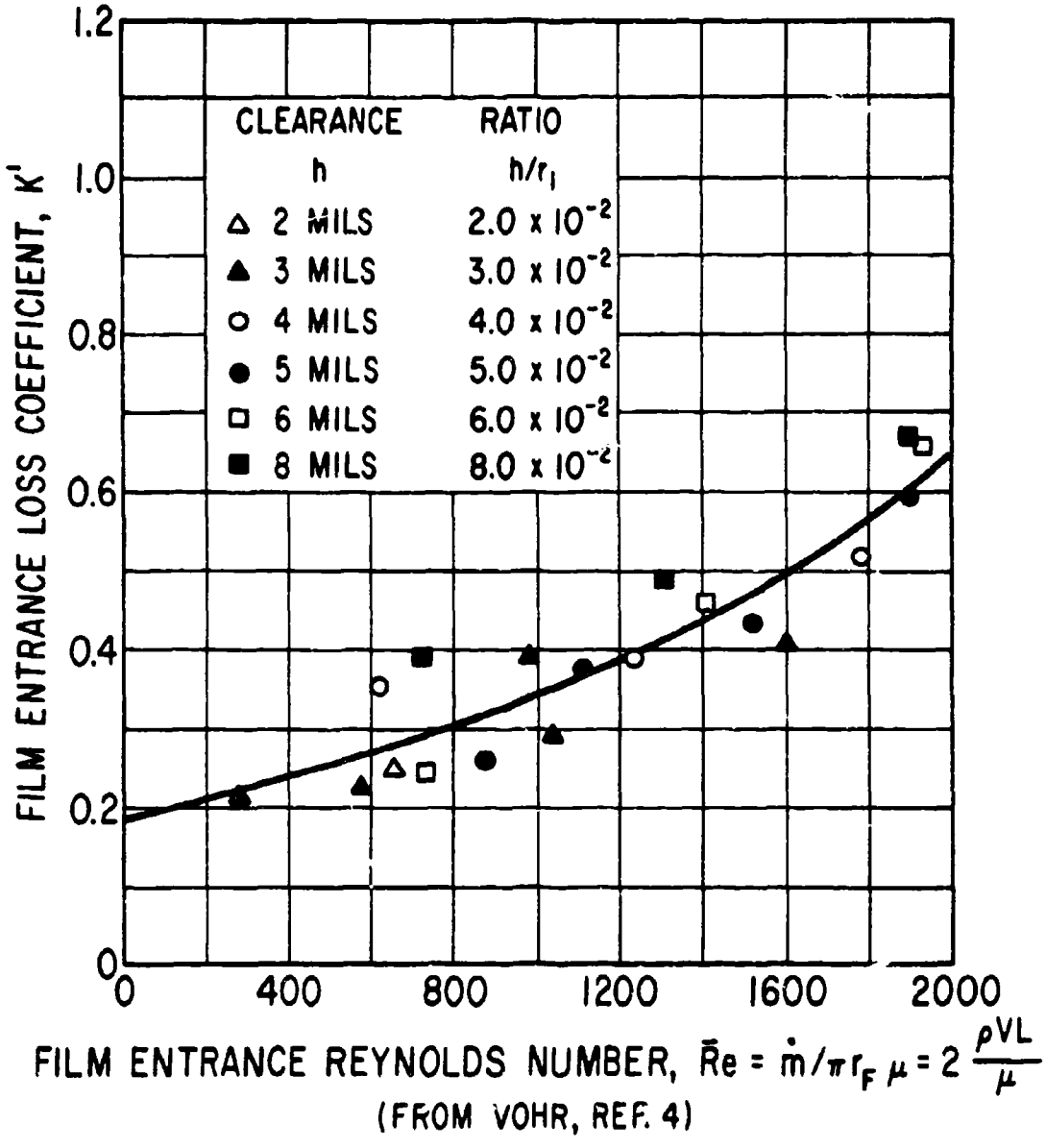

Fig. 2 Loss Coefficient versus Film Entrance Reynolds Number

MTI-6619

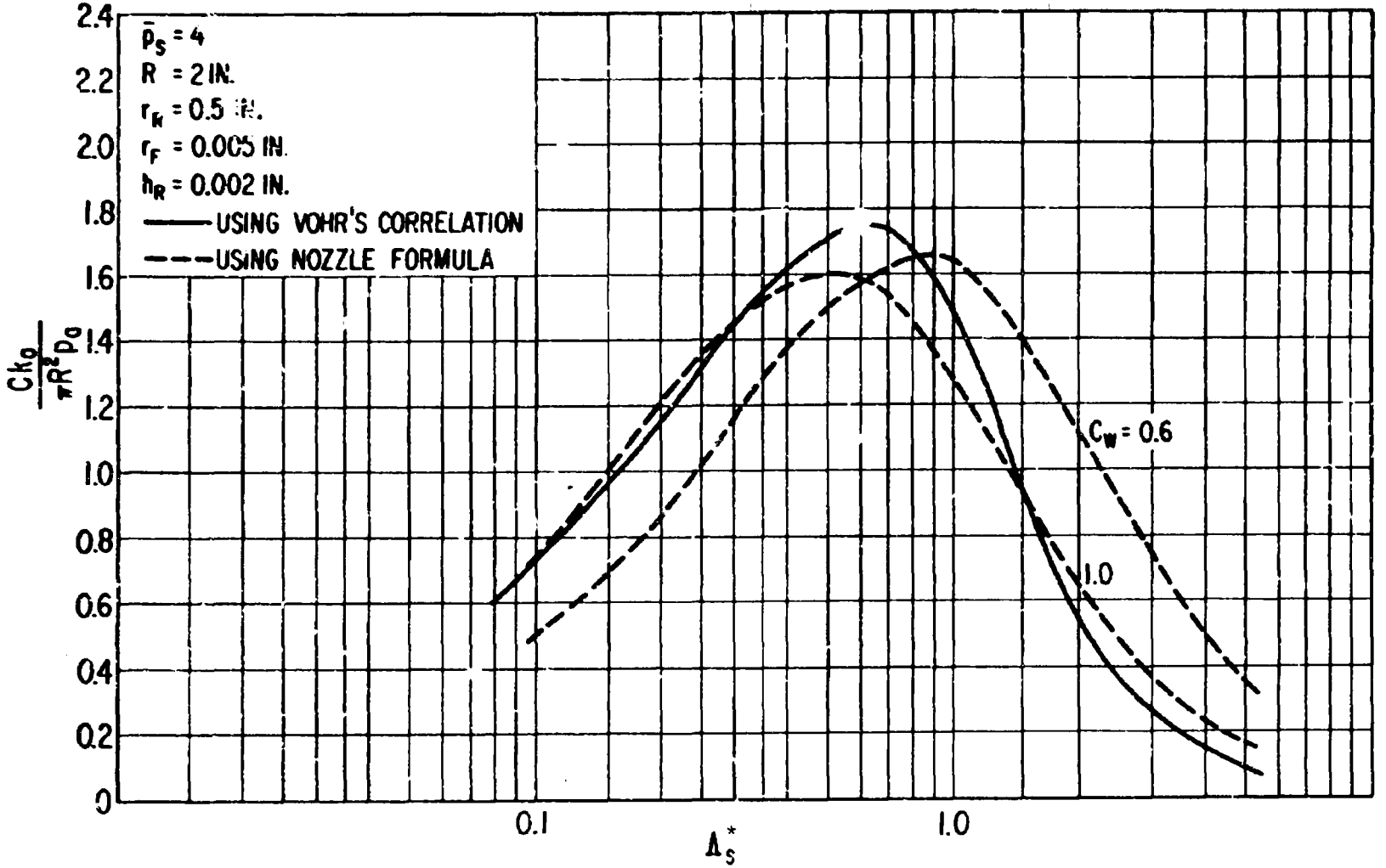

Fig. 5 Static Stiffness versus Λ_s^* at $\bar{p}_s = 4$

MTI-6582

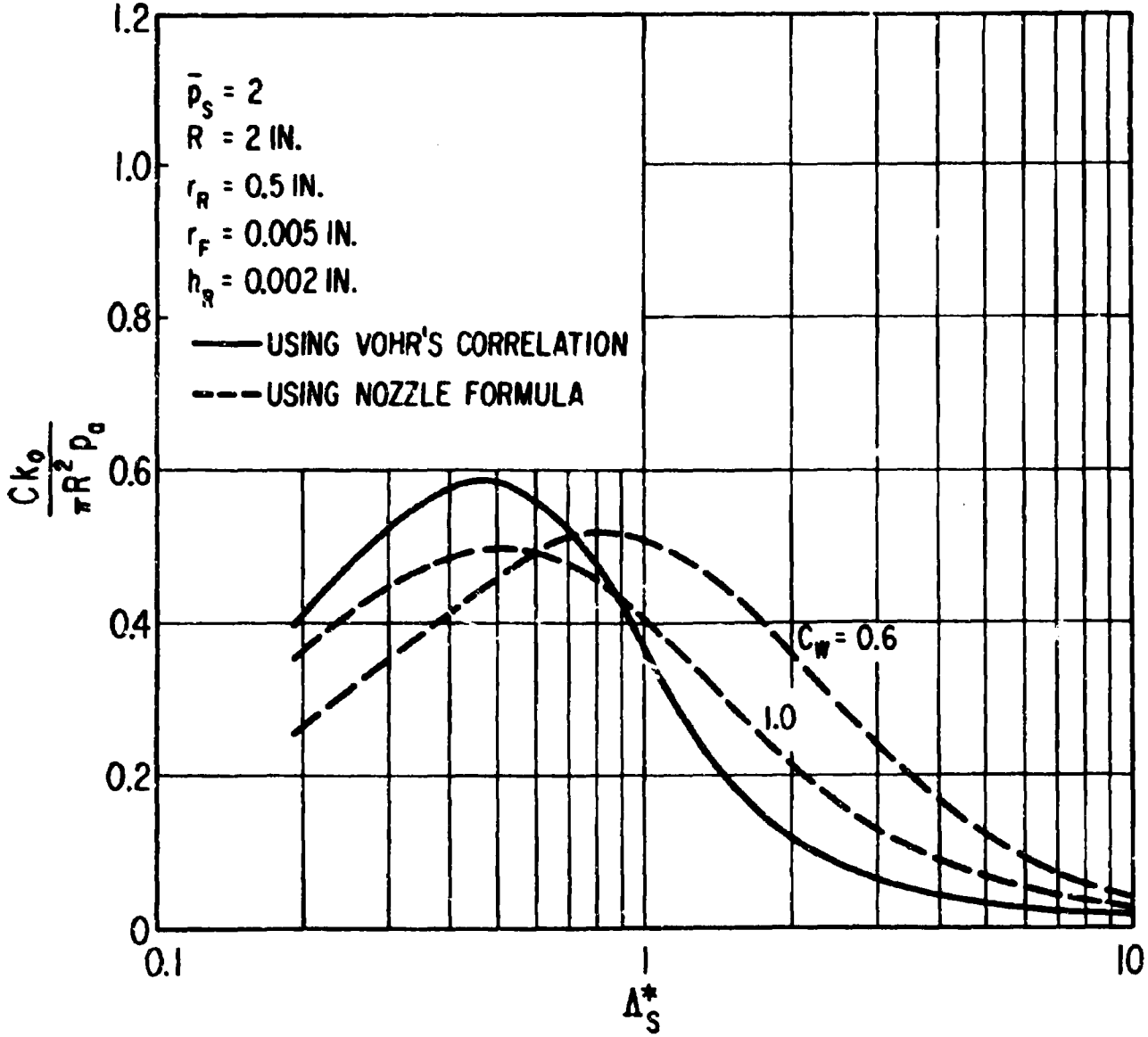

Fig. 4 Static Stiffness versus Λ_s^* at $\bar{p}_s = 2$

MTI-6589

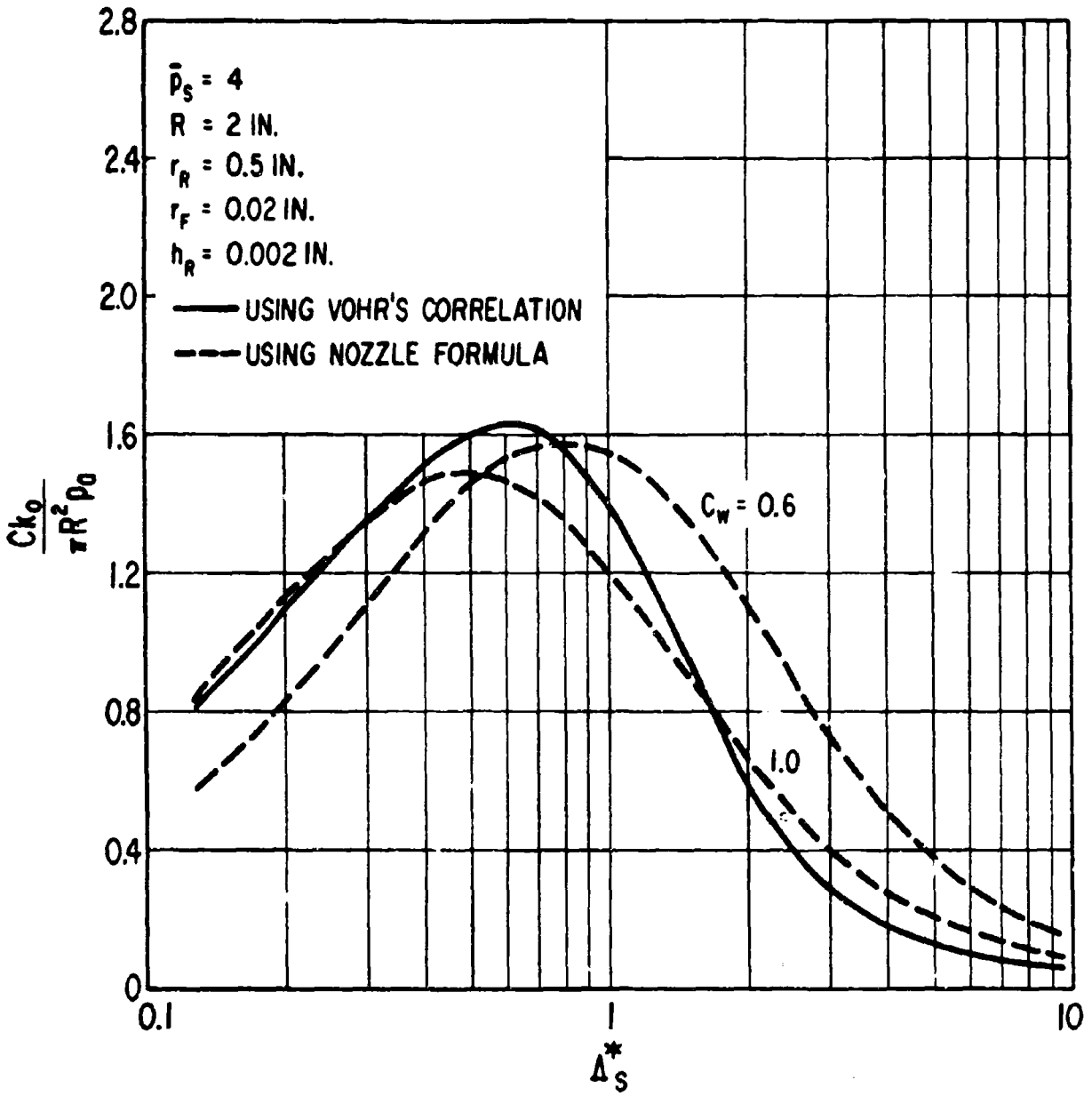

Fig. 5 Static Stiffness versus Λ_s^* with r_F = 0.02 in.

MTI-6588

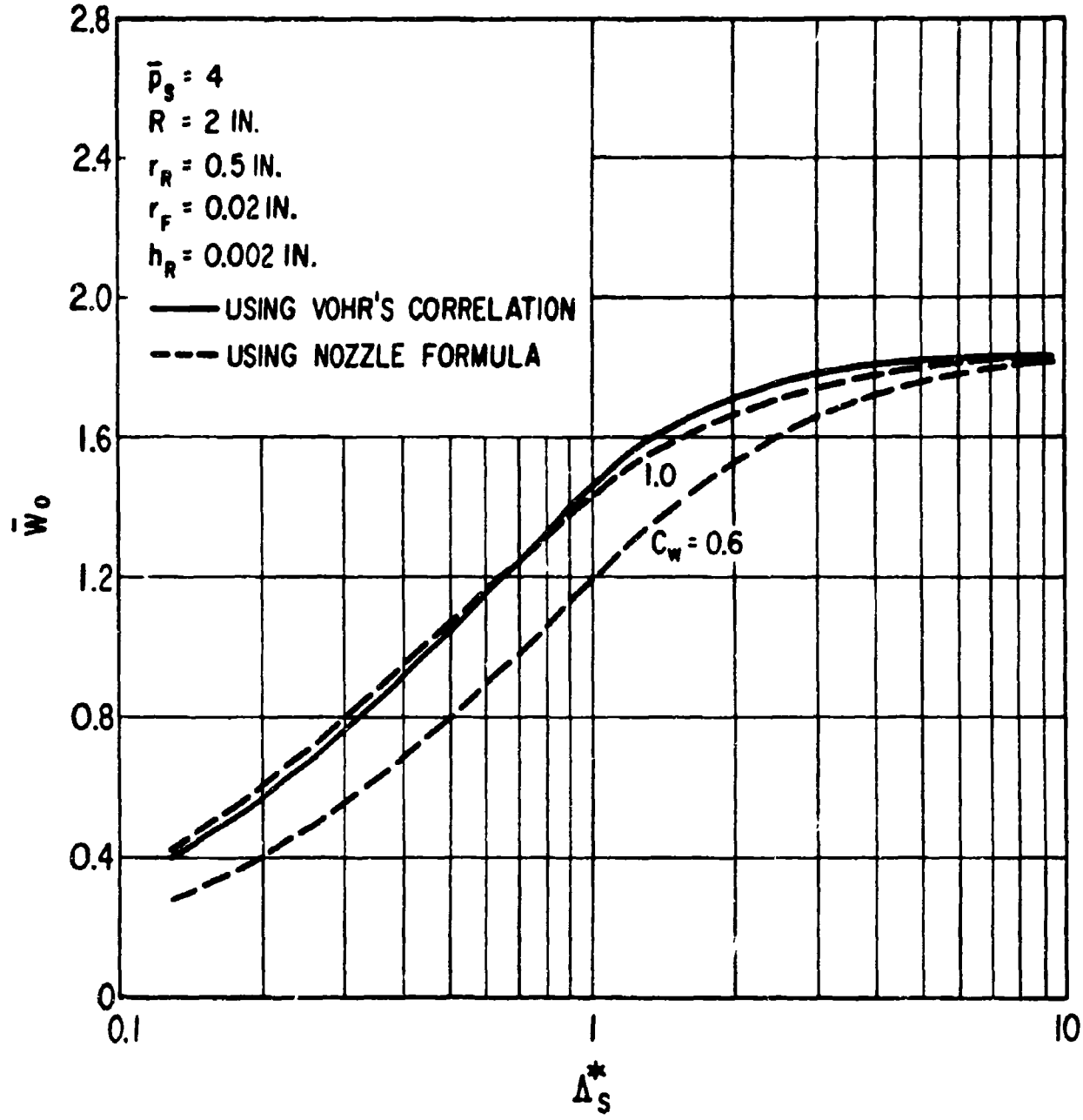

Fig. 6 Load Capacity versus Λ_s^*

AII-6581

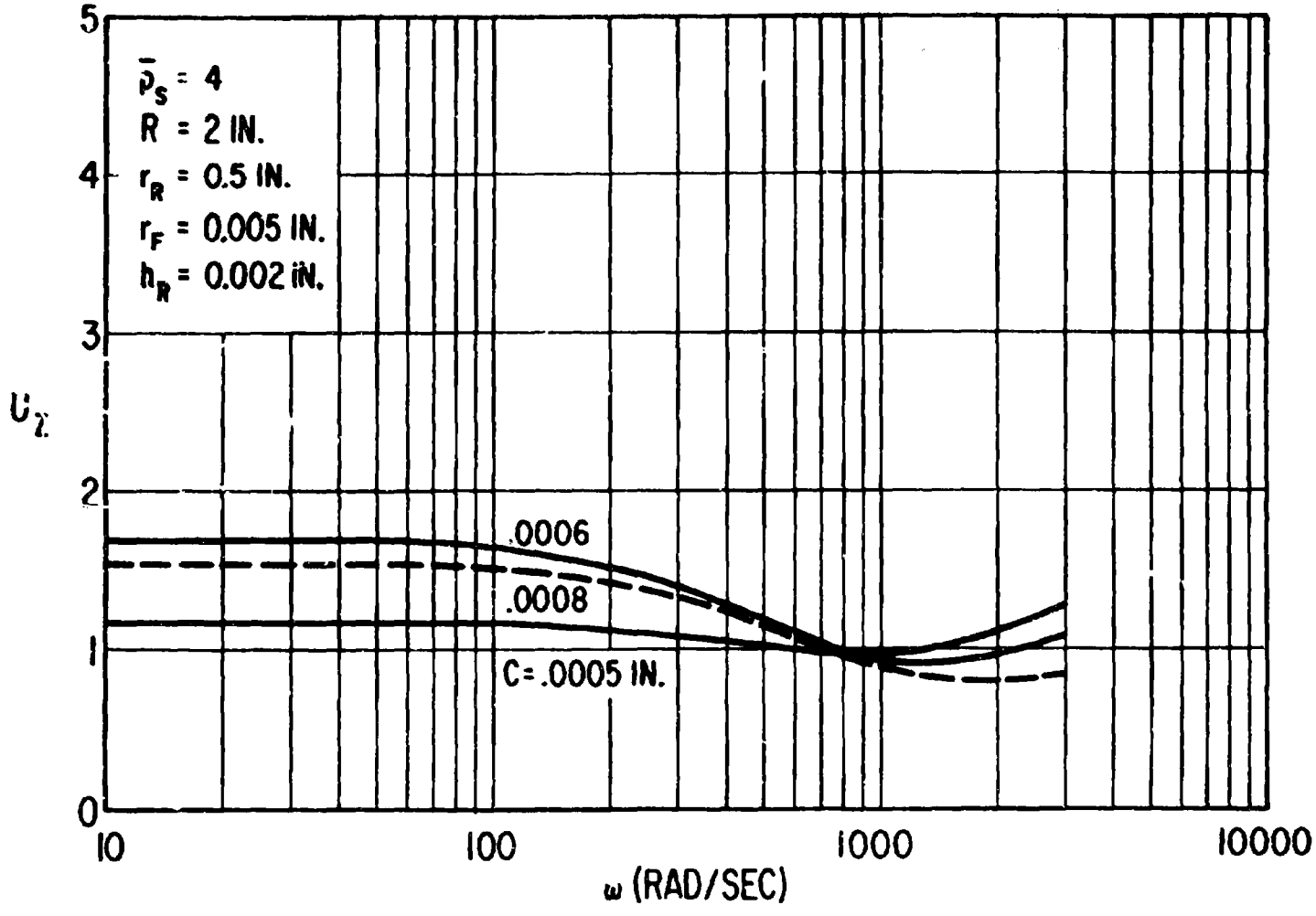

Fig. 7 Dynamic Stiffness U_z versus Frequency ω

MTI-6585

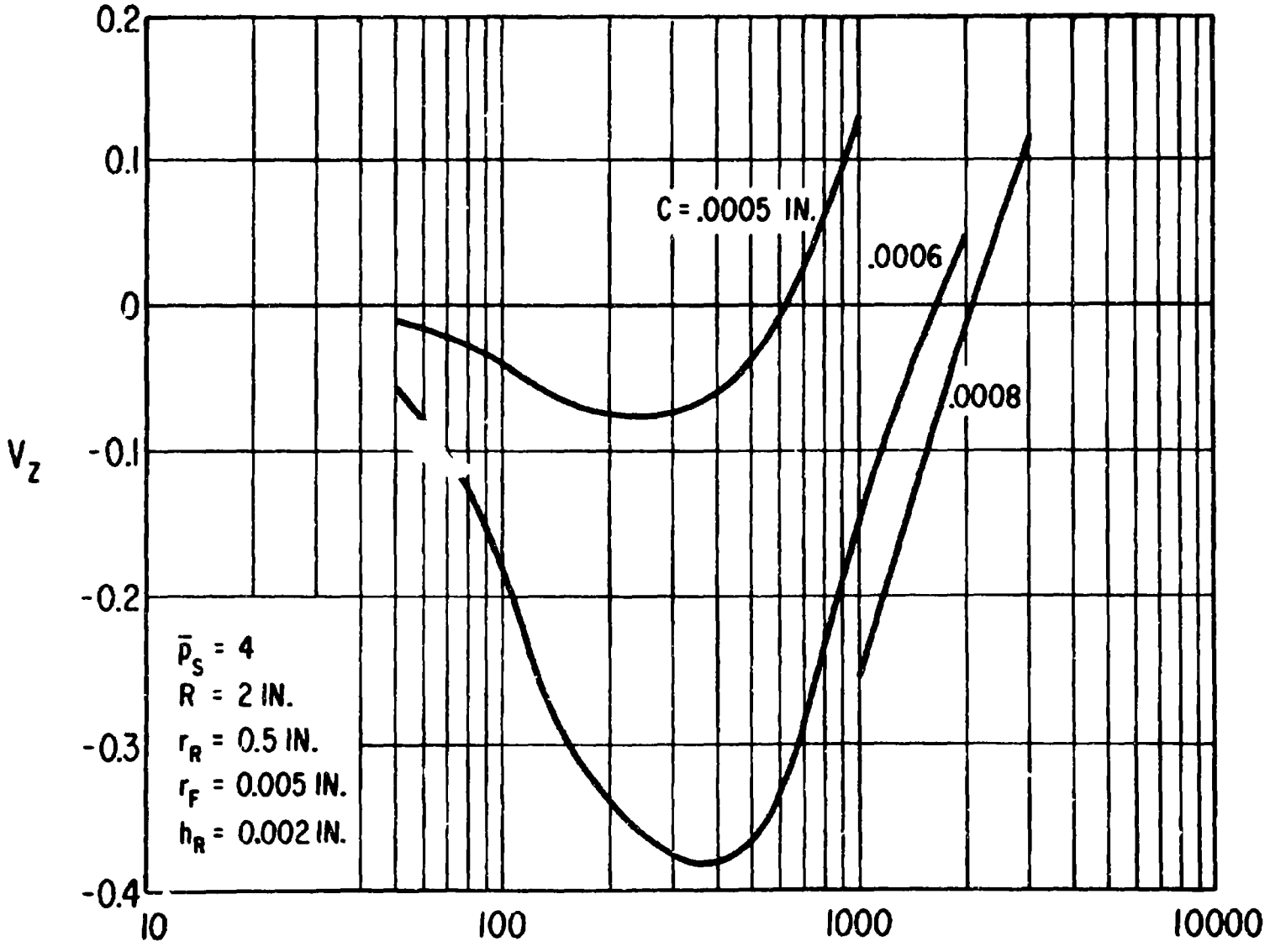

Fig. 8 Dynamic Damping V_z versus Frequency ω

MTI-6586

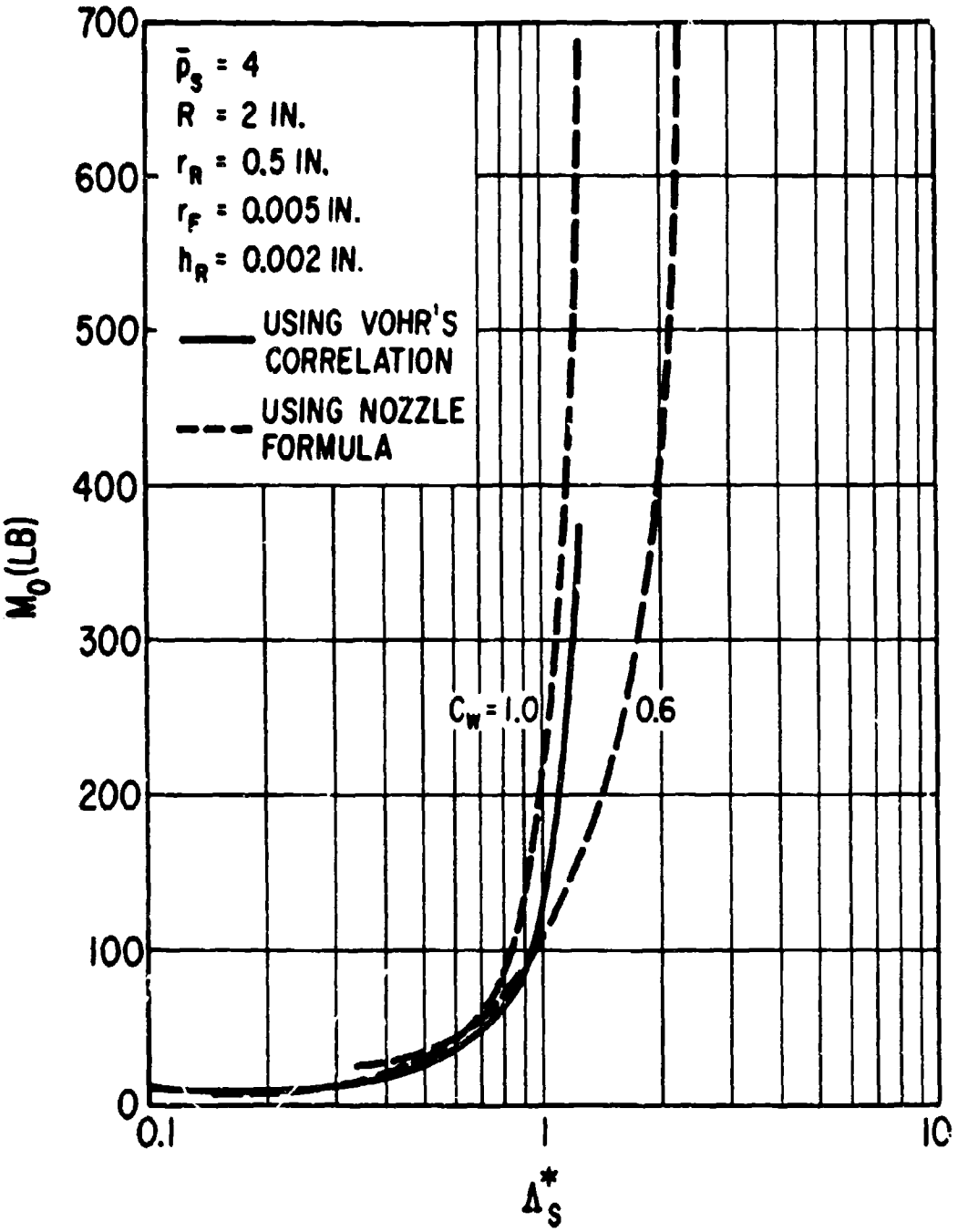

Fig. 9. Critical Mass versus Λ_s^*

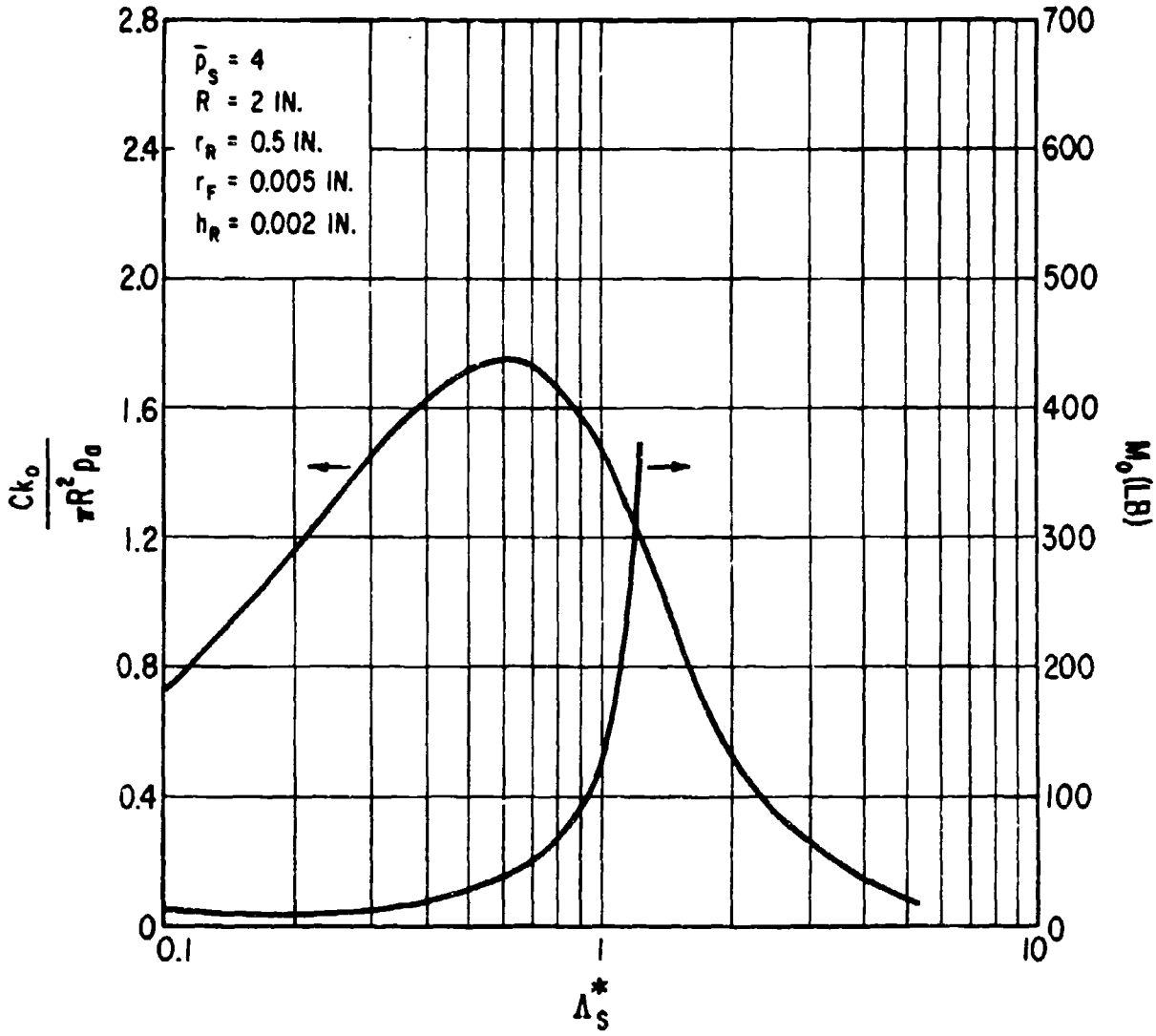

Fig. 10 Critical Mass and Static Stiffness versus Λ_s^* using Vohr's Correlation

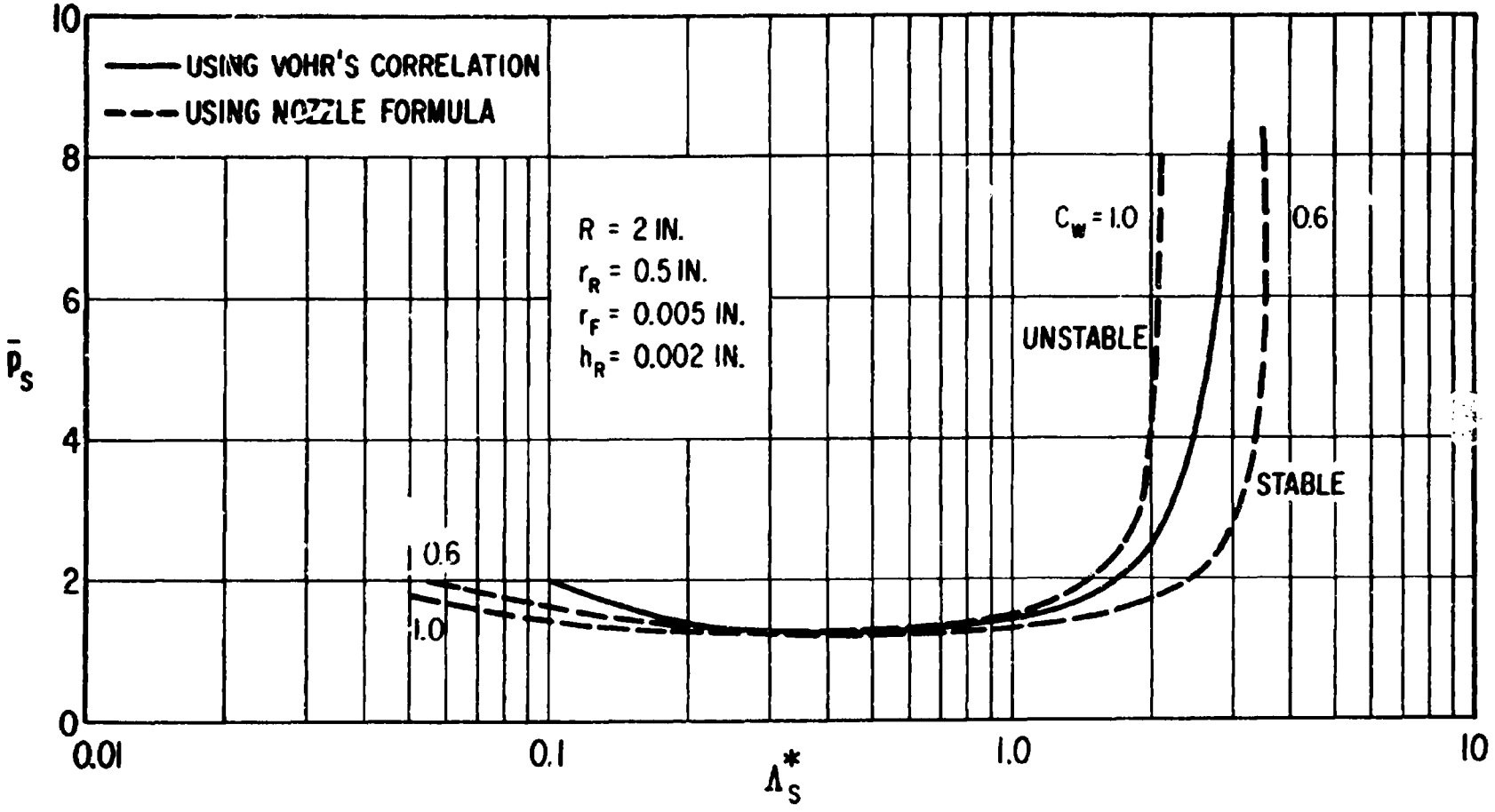

Fig. 11 Stability Map at a Fixed Pocket Depth

MTI-6583

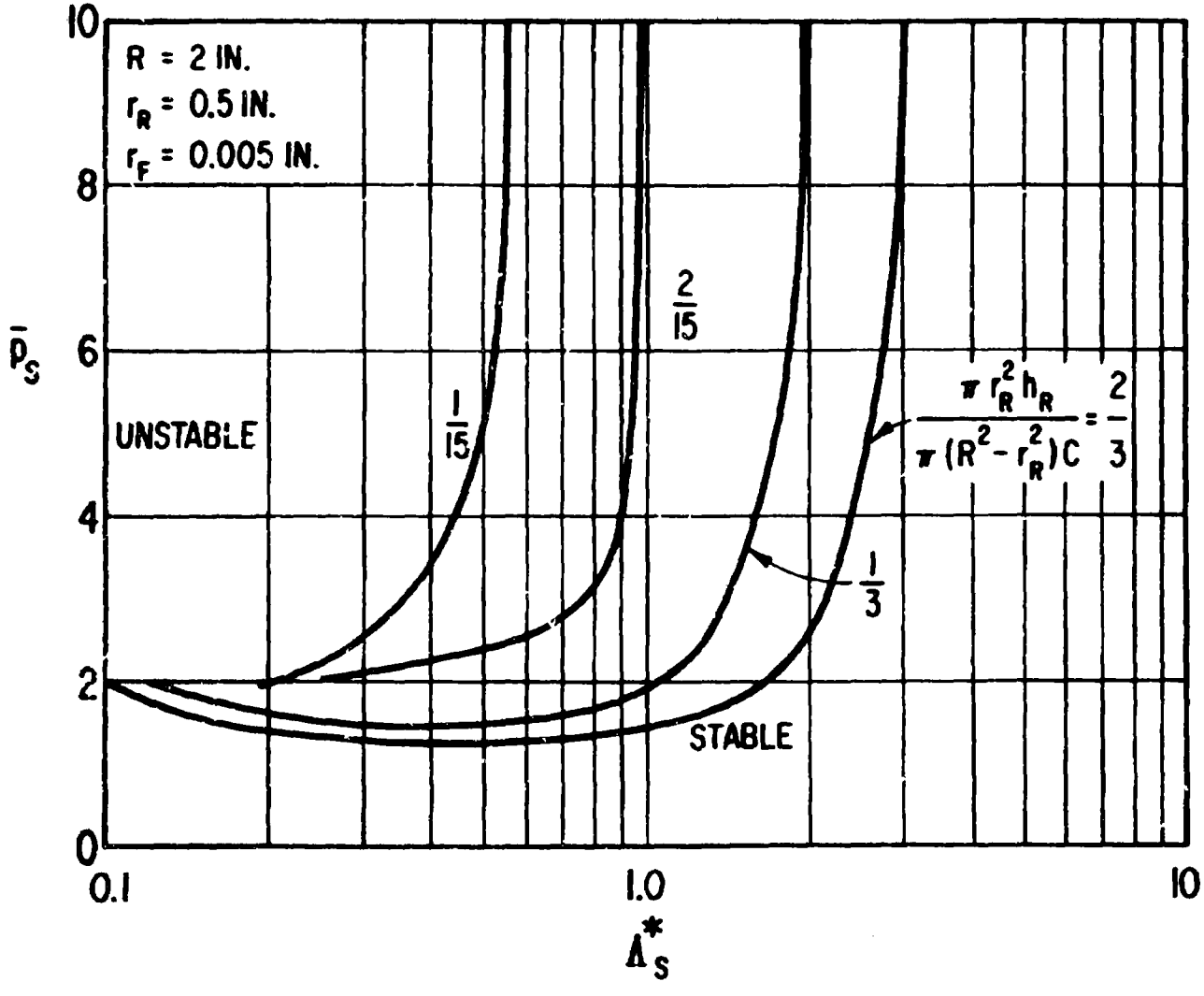

Fig. 12 Stability Map for Various Film-to-Pocket Volume Ratio

MTI-6587

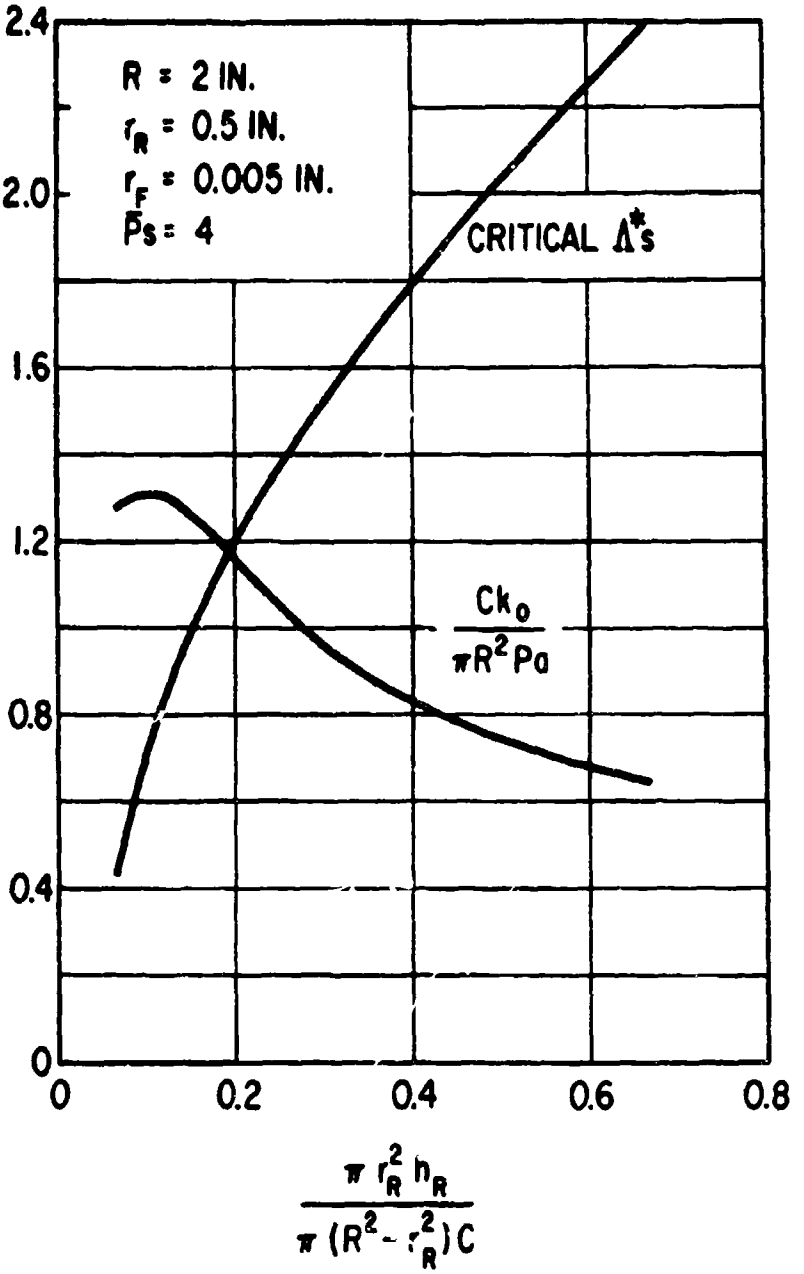

Fig. 13 Static Stiffness versus Film-to-Pocket Volume Ratio at the Respective Critical Λ^*_S

MTI-6584

UNCLASSIFIED

Security Classification

DOCUMENT CONTROL DATA - R&D

(Security classification of title, body of abstract and indexing annotation must be entered when the overall report is classified)

1. ORIGINATING ACTIVITY (Corporate author)	2a. REPORT SECURITY CLASSIFICATION
Mechanical Technology Incorporated 968 Albany-Shaker Road Latham, New York 12110	Unclassified 2b. GROUP

3. REPORT TITLE

Refined Solution of Pneumatic Hammer Instability of Inherently Compensated Hydrostatic Thrust Gas Bearings.

4. DESCRIPTIVE NOTES (Type of report and inclusive dates)

Technical Topical Report - March 1969

5. AUTHOR(S) (Last name, first name, initial)

Chiang, T.
Pan, Coda H. T.

6. REPORT DATE	7a. TOTAL NO. OF PAGES	7b. NO. OF REFS
March 1969	52	13

8a. CONTRACT OR GRANT NO.	9a. ORIGINATOR'S REPORT NUMBER(S)
Nonr 3730(00) b. PROJECT NO. NR-062-317 c. d	MTI 69TR23 9b. OTHER REPORT NO(S) (Any other numbers that may be assigned this report)

10. AVAILABILITY/LIMITATION NOTICES

Distribution of this document is unlimited.

11. SUPPLEMENTARY NOTES	12. SPONSORING MILITARY ACTIVITY
	U.S. Navy Department Office of Naval Research

13. ABSTRACT

An externally-pressurized gas thrust bearing was analyzed for both static and dynamic characteristics. The bearing is fed through an inherently compensated restrictor into a shallow pocket. The analysis gave special attentions to the significance of the recent finding of restrictor flow ~~(Ref. 4)~~, the trade-off consideration between static stiffness and stability margin, and the effects of the pocket depth.

DD FORM 1 JAN 64 1473

Security Classification

UNCLASSIFIED

Security Classification

DOCUMENT CONTROL DATA - R&D

(Security classification of title, body of abstract and indexing annotation must be entered when the overall report is classified)

1. ORIGINATING ACTIVITY *(Corporate author)*
Mechanical Technology Incorporated
968 Albany-Shaker Road
Latham, New York 12110

2a. REPORT SECURITY CLASSIFICATION
Unclassified

2b GROUP

3. REPORT TITLE
Refined Solution of Pneumatic Hammer Instability of Inherently Compensated Hydrostatic Thrust Gas Bearings.

4. DESCRIPTIVE NOTES *(Type of report and inclusive dates)*
Technical Topical Report - March 1969

5. AUTHOR(S) *(Last name, first name, initial)*
Chiang, T.
Pan, Coda H. T.

6. REPORT DATE	7a. TOTAL NO. OF PAGES	7b. NO. OF REFS
March 1969	52	13

8a. CONTRACT OR GRANT NO.	9a. ORIGINATOR'S REPORT NUMBER(S)
Nonr 3730(00)	MTI 69TR23
b. PROJECT NO. NR-062-317	
c.	9b. OTHER REPORT NO(S) *(Any other numbers that may be assigned this report)*
d.	

10. AVAILABILITY/LIMITATION NOTICES
Distribution of this document is unlimited.

11. SUPPLEMENTARY NOTES	12. SPONSORING MILITARY ACTIVITY
	U.S. Navy Department Office of Naval Research

13. ABSTRACT

An externally-pressurized gas thrust bearing was analyzed for both static and dynamic characteristics. The bearing is fed through an inherently compensated restrictor into a shallow pocket. The analysis gave special attentions to the significance of the recent finding of restrictor flow ~~(Ref. 4)~~, the trade-off consideration between static stiffness and stability margin, and the effects of the pocket depth ( ).

DD FORM 1 JAN 64 1473

Security Classification